

CHAPTER IV

RESULTS AND DISCUSSION

A. Extraction of Active Constituents from *Garcinia mangostana*

The crude extract of *Garcinia mangostana* was prepared by macerating two kilograms of the dried fruit hulls with hexane for extraction of non polar substances. After removal of the hexane extract, the marc was further extracted with ethyl acetate. The ethyl acetate extract was obtained as brownish viscous liquid which was concentrated by using a rotary evaporator. Then the extract was crystallized into yellow crystal and ground into fine powder for further studies (Figure 22). The weight of final yield was 57.65 g, which was calculated as 2.88% yield.



Figure 22 Photograph of *Garcinia mangostana* extract

B. Determination of Active Constituents from *Garcinia mangostana*

1. Differential Scanning Calorimetric (DSC) Method

Differential scanning calorimetric method was used in this study to detect the melting point of the extract. The weight of 3.14 mg of the extract was placed into an

aluminum pan and the run was performed at the heating rate 10 °C/min in the temperature range of 0-250 °C. The DSC thermogram of the extract showed an endothermic melting peak at 179.69 °C (Figure 23). This melting point was conformed to the melting point of mangostin which was reported as 181.6-182.6 °C (Budavari, 2001).

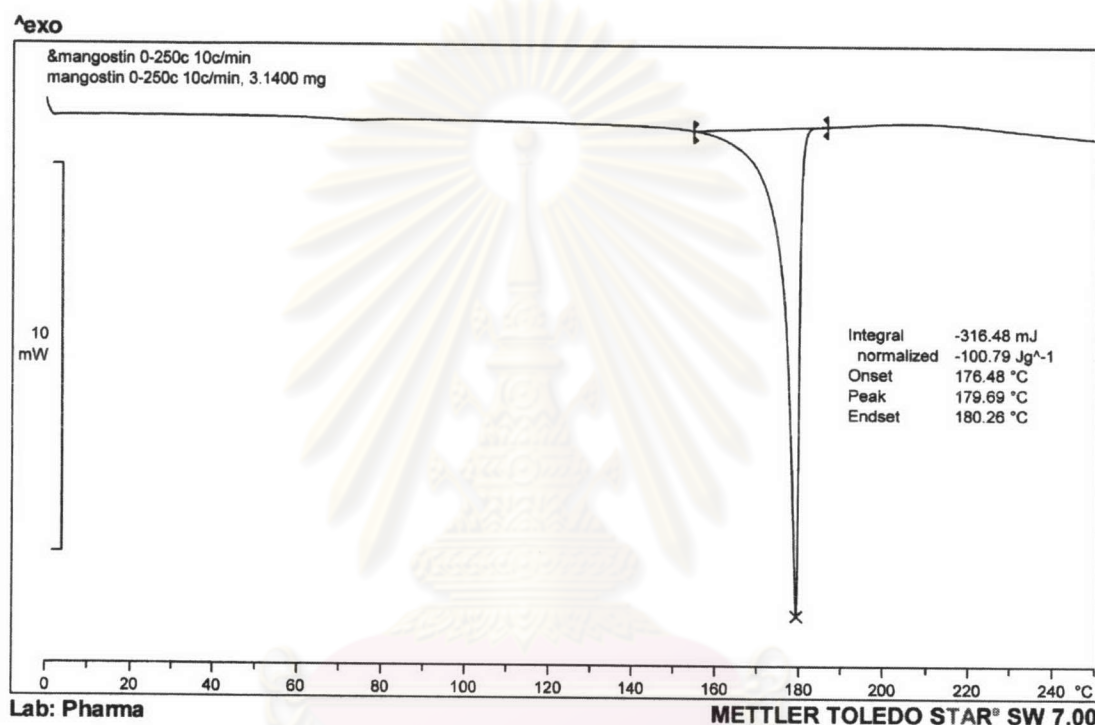


Figure 23 DSC thermogram of *Garcinia mangostana* extract

2. Thin Layer Chromatographic (TLC) Method

The isolated compound from dried fruit hulls extract was identified by TLC. The chromatogram of the compound was compared to the standard mangostin as shown in Figure 24. In this chromatogram, the R_f value of the extract was equal to the standard mangostin at the value of 0.60. Based on this data, the extract corresponded to mangostin.



Figure 24 TLC chromatogram of (a) standard mangostin and (b) *Garcinia mangostana* extract

3. High Performance Liquid Chromatographic (HPLC) Method

The developed HPLC system was applied to analyze the extract from dried fruit hulls of *Garcinia mangostana*. It was found that the extract had similar chromatogram to the standard mangostin. However, in the same concentration the extract gave the peak area ratio of $80.89 \pm 0.70\%$ of the standard mangostin.

3.1 Validation of HPLC Method

The validation of analytical method is the process by which it is established that the performance characteristics of the method meet the requirements for the intended analytical applications. The performance characteristics are expressed in terms of analytical parameters. For HPLC assay validation, these include specificity, linearity, accuracy and precision.

3.1.1 Specificity

The specificity of an analytical method is its ability to measure the analyte accurately and with specificity in the presence of other components in the sample.

The internal standard technique was performed by determining the peak area ratio of mangostin to clotrimazole (internal standard) to give the complete separation, appropriate resolution and sharp peaks of all components. The methanol-water mixture of 85% by volume was used as the mobile phase. The typical chromatograms of blank solution, internal standard solution, mangostin standard solution and *Garcinia mangostana* extract solution are shown in Figures 25-30.

The retention times of blank solution, internal standard solution, mangostin standard solution and *Garcinia mangostana* extract solution were around 3.054, 6.037, 14.557 and 14.520 min, respectively. In addition, there was no interference from other components in the chromatogram.

3.1.2 Linearity

The linearity of an analytical method is its ability to elicit test results that are directly, or by a well-defined mathematical transformation, proportional to the concentration of analyte in samples within a given range. The linearity is usually expressed in terms of the variance around the slope of the regression line calculated according to an established mathematical relationship from test results obtained by the analysis of samples with varying concentrations of analyte. The calibration curve data of mangostin standard solutions are shown in Table 6. The plot of mangostin concentrations versus the peak area ratios of mangostin and its internal standard (Figure 31) illustrated the linear correlation in the concentration range studied of 5-50 $\mu\text{g/ml}$. The coefficient of determination (R^2) of this line was 0.9998. These results indicated that HPLC method was acceptable for quantitative analysis of mangostin in the range studied.

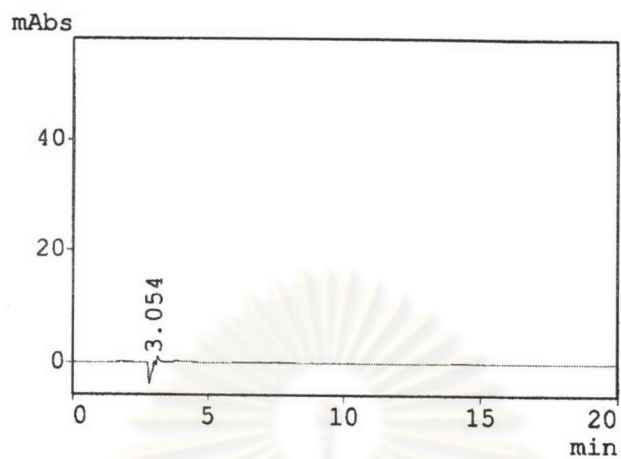


Figure 25 HPLC Chromatogram of blank solution

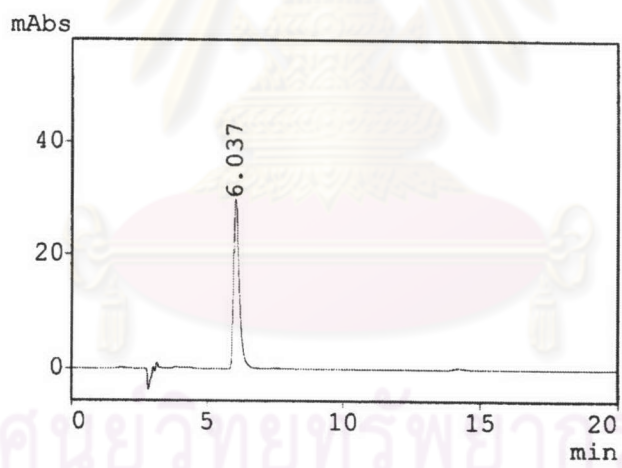


Figure 26 HPLC Chromatogram of internal standard solution (clotrimazole)

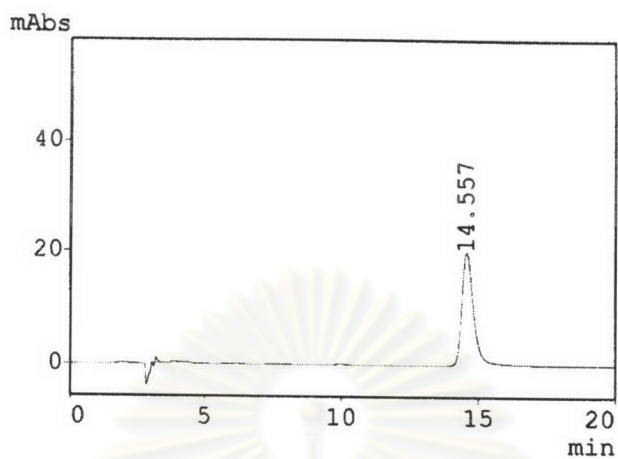


Figure 27 HPLC Chromatogram of mangostin standard solution

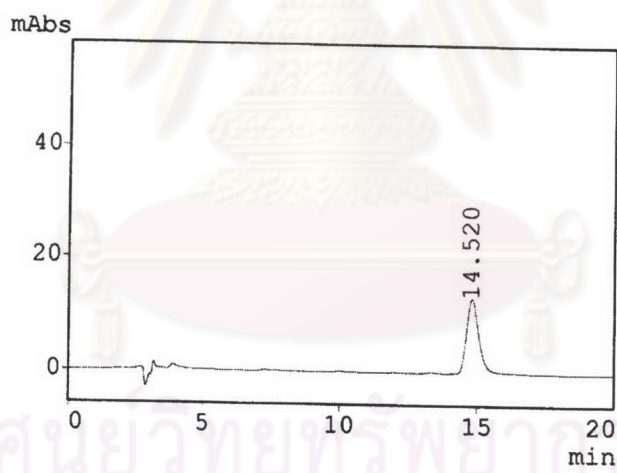


Figure 28 HPLC Chromatogram of *Garcinia mangostana* extract solution

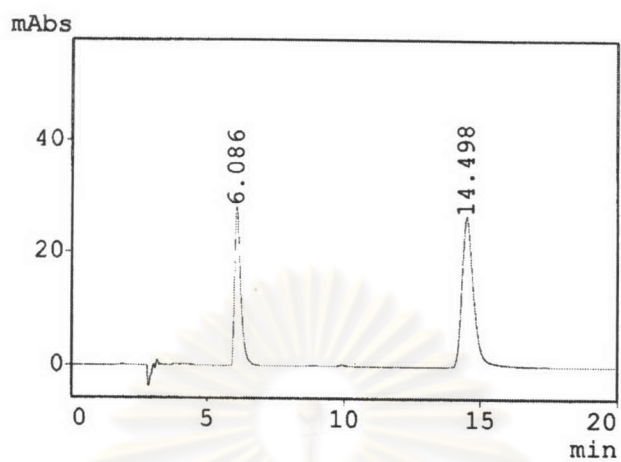


Figure 29 HPLC Chromatogram of mixture of mangostin and internal standard

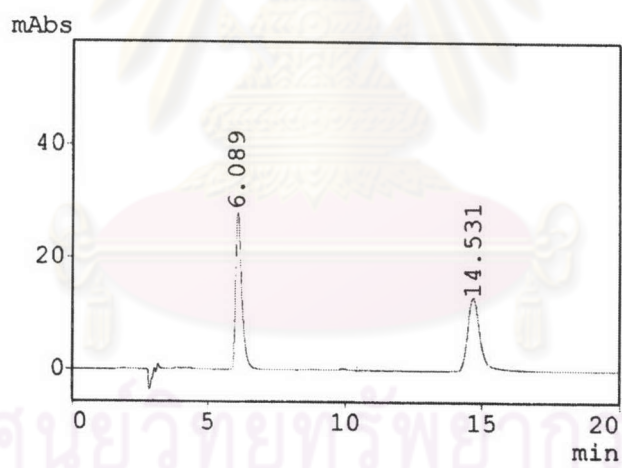


Figure 30 HPLC Chromatogram of mixture of the extract and internal standard

Table 6 Data for calibration curve of mangostin by HPLC method

Concentration ($\mu\text{g/ml}$)	Peak area ratio			Mean	SD	%CV
	Set 1	Set 2	Set 3			
5	0.4261	0.4301	0.4295	0.4286	0.0022	0.50
10	0.8168	0.8112	0.8154	0.8145	0.0029	0.36
20	1.6615	1.6690	1.6725	1.6677	0.0056	0.34
30	2.5721	2.5802	2.5756	2.5760	0.0041	0.16
40	3.4202	3.4111	3.4175	3.4163	0.0047	0.14
50	4.2541	4.2509	4.2455	4.2502	0.0043	0.10
R^2	0.9998	0.9997	0.9998	0.9998	-	-

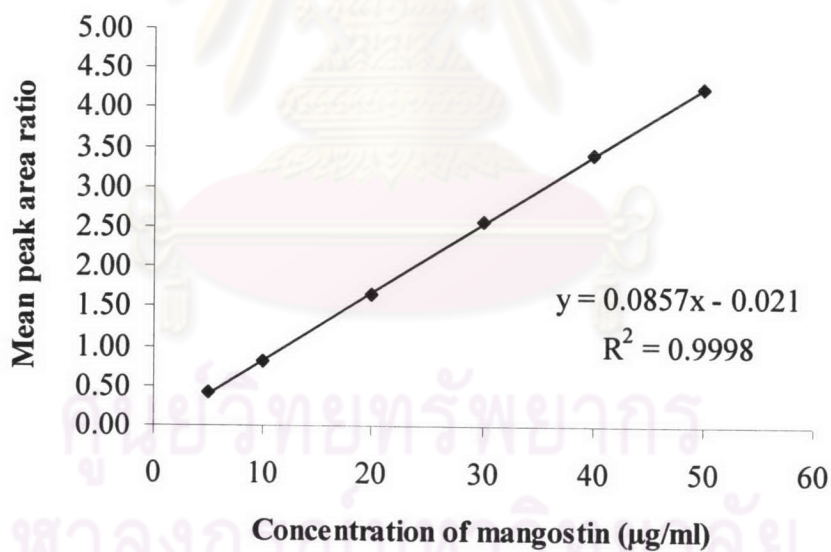


Figure 31 Calibration curve of mangostin by HPLC method

3.1.3 Accuracy

The determination of accuracy was performed by analyzing five sets of three standard solutions (low, medium, high). The inversely estimated concentrations and percentages of analytical recovery of each drug concentration are shown in Table 7 and Table 8, respectively. All percentages of analytical recovery were in the range of 99.79-101.21%, which indicated that this method could be used for analysis of mangostin in all concentrations studied with high accuracy.

Table 7 The inversely estimated concentrations of mangostin by HPLC method

Concentration ($\mu\text{g/ml}$)	Inversely estimated concentration ($\mu\text{g/ml}$)					Mean \pm SD
	Set 1	Set 2	Set 3	Set 4	Set 5	
5	5.0450	5.0345	5.0579	5.0895	5.0380	5.0530 \pm 0.02
25	25.1836	25.2738	25.2586	25.4766	25.3148	25.3015 \pm 0.11
50	49.8768	49.8205	49.9120	49.8709	49.9987	49.8958 \pm 0.07

Table 8 The percentage of analytical recovery of mangostin by HPLC method

Concentration ($\mu\text{g/ml}$)	% Analytical recovery					Mean \pm SD
	Set 1	Set 2	Set 3	Set 4	Set 5	
5	100.90	100.69	101.16	101.79	100.76	101.06 \pm 0.45
25	100.73	101.10	101.03	101.91	101.26	101.21 \pm 0.44
50	99.75	99.64	99.82	99.74	100.00	99.79 \pm 0.13

3.1.4 Precision

The precision of an analytical method is the degree of agreement among individual test results when the method is applied repeatedly to multiple samplings of a homogeneous sample. The precision of an analytical method is usually expressed as the standard deviation or relative standard deviation (coefficient of variation) of a series of measurements.

Table 9 and Table 10 illustrate the data of within run precision and between run precision, respectively. All coefficient of variation values were small, 0.13-0.45% and 0.20-1.13%, respectively. The coefficient of variation of an analytical method should generally be less than 2%. Therefore, the HPLC method was precise for quantitative analysis of mangostin in the range studied.

Table 9 Data of within run precision by HPLC method

Concentration ($\mu\text{g/ml}$)	Peak area ratio					Mean	SD	%CV
	Set 1	Set 2	Set 3	Set 4	Set 5			
5	0.4221	0.4212	0.4232	0.4259	0.4215	0.4228	0.0019	0.45
25	2.1403	2.1480	2.1467	2.1653	2.1515	2.1504	0.0093	0.43
50	4.2471	4.2423	4.2501	4.2466	4.2575	4.2487	0.0056	0.13

Table 10 Data of between run precision by HPLC method

Concentration ($\mu\text{g/ml}$)	Peak area ratio					Mean	SD	%CV
	Set 1	Set 2	Set 3	Set 4	Set 5			
5	0.4301	0.4279	0.4211	0.4272	0.4344	0.4281	0.0048	1.13
25	2.1541	2.1552	2.1652	2.1460	2.1406	2.1522	0.0094	0.44
50	4.2470	4.2455	4.2445	4.2626	4.2601	4.2519	0.0087	0.20

In conclusion, the analysis of mangostin by HPLC method developed in this study showed good specificity, linearity, accuracy and precision. Thus this method was used for the determination of the content of mangostin in the study.

C. Preparation of Monoglyceride-Based Drug Delivery System

1. Monoglyceride-Based Drug Delivery System

Monoglyceride-based drug delivery systems were developed by the ability of glyceryl monooleate and triglycerides to form liquid crystals in contact with water.

Liquid crystalline phases were formed under the conditions used in this study. Partial phase diagrams of these liquid crystalline systems are displayed in Figures 32-34. In this study, partial phase diagrams were used because the outer area could not give the 1-phase liquid crystals. The ternary phase diagram of glyceryl monooleate-sesame oil-water system gave the area of one-phase liquid crystalline more than other two systems using soybean oil and olive oil. Although the differences in phase behavior were found by using various oils, these differences were generally small. The phase behavior of these systems is similar to the system (monoolein-sesame oil-water) studied by Norling et al. (1992). However, the precise locations of the phase boundaries in the diagram differed slightly.

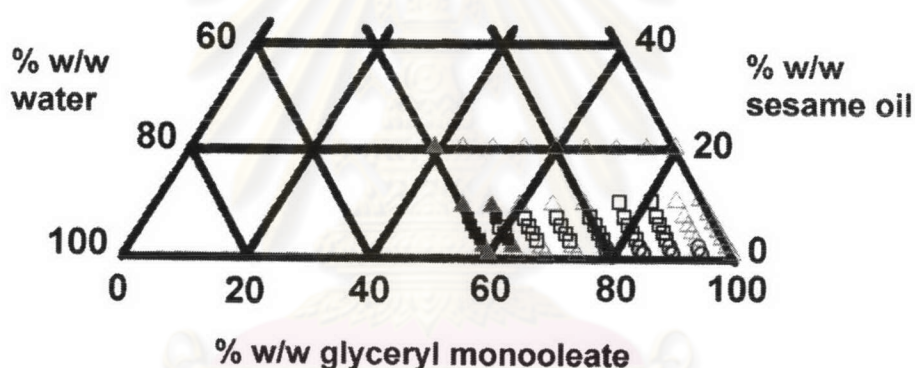


Figure 32 Ternary phase diagram of glyceryl monooleate-sesame oil-water system; (O) lamellar phase (L_{α}); (□) reversed hexagonal phase (H_{II}); (■) reversed hexagonal phase (H_{II}) + aqueous; (Δ) isotropic, 1-phase; and (▲) isotropic, 2-phase

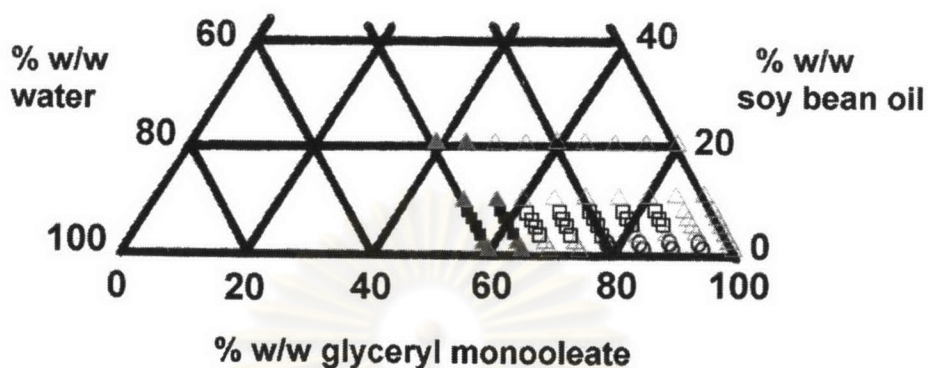


Figure 33 Ternary phase diagram of glyceryl monooleate-soybean oil-water system; (O) lamellar phase (L_{α}); (□) reversed hexagonal phase (H_{II}); (■) reversed hexagonal phase (H_{II}) + aqueous; (Δ) isotropic, 1-phase; and (\blacktriangle) isotropic, 2-phase

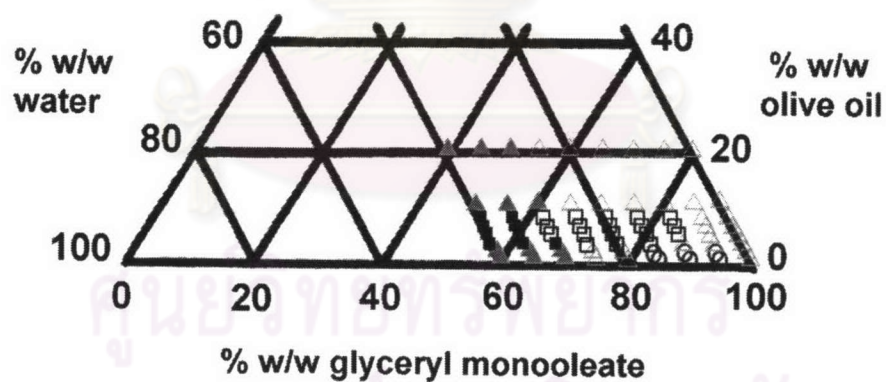


Figure 34 Ternary phase diagram of glyceryl monooleate-olive oil-water system; (O) lamellar phase (L_{α}); (□) reversed hexagonal phase (H_{II}); (■) reversed hexagonal phase (H_{II}) + aqueous; (Δ) isotropic, 1-phase; and (\blacktriangle) isotropic, 2-phase

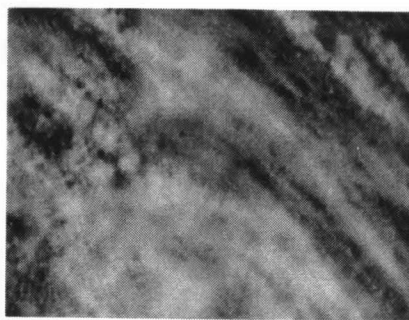
2. Physical Characterization

2.1 Polarized Light Microscopy

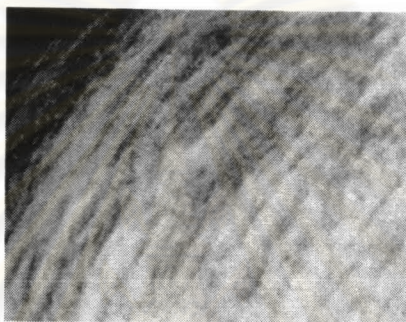
The formation and structure of liquid crystalline phases were identified under polarized light microscopy. Liquid crystals formed by glyceryl monooleate, water and triglycerides content not more than 4% had liquid crystal structures conformable to a lamellar structure established by Makai et al. (2003) as shown in Figure 35. When increasing the triglycerides content from 6% to 15%, liquid crystal structures were changed which structure similar to a reversed hexagonal phase observed by Geraghty et al. (1996) (Figure 36). The difference in triglycerides, sesame oil, soybean oil or olive oil, showed the same pattern of liquid crystalline phases under polarized light microscope. These results might be from the small amount of triglycerides compared to glyceryl monooleate which was the main component and had the ability to form liquid crystals. In this study, there had been a dark background under polarized light microscope which could not be identified to cubic phase or reversed micellar by this method. From the results, the formation and structure of liquid crystalline phases depended on the characteristic of the amphiphilic compounds and the ratio of the components in the phase diagram.

2.2 Physical Stability

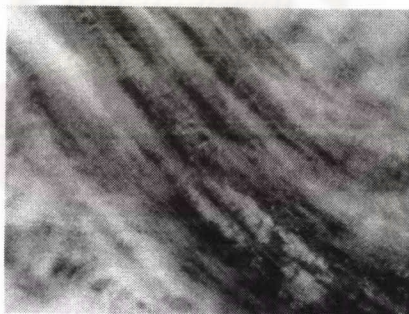
The samples that could form reversed hexagonal phases were selected for this study due to their favorable sustained release (Norling et al., 1992). Under the heating-cooling cycle, the samples with water content lower than 30% did not show any changes in physical appearances. While the samples with water content 35% showed phase separation after the stress condition. The reason is that increasing water content, it tends to be two-phase separation according to the phase diagram.



(a)



(b)



(c)

Figure 35 Polarizing microscopic images of the lamellar phases; (a) system containing sesame oil; (b) system containing soybean oil; and (c) system containing olive oil, as observed at $\times 100$ magnification



(a)



(b)



(c)

Figure 36 Polarizing microscopic images of the reversed hexagonal phases; (a) system containing sesame oil; (b) system containing soybean oil; and (c) system containing olive oil, as observed at $\times 100$ magnification

D. Formulation of *Garcinia mangostana* Extract Monoglyceride-Based Drug Delivery System

The monoglyceride-based drug delivery systems were composed of mixtures of monoglyceride, triglycerides from vegetable oils and water. The relative amount of monoglyceride and vegetable oil in the composition for formulation of the reversed hexagonal liquid crystalline phase may vary over a considerable range. Generally, the vegetable oil is present in an amount sufficient to improve the flow characteristics of the composition upon release from the dosing device and induce the formation of a stable reversed hexagonal liquid crystalline phase upon contact with an aqueous liquid. Generally, the vegetable oil and monoglyceride are presented in a weight ratio of 1:99 to 30:70 vegetable oil to monoglyceride, most preferably from 5:95 to 15:85, based upon the combined weight of the monoglyceride and vegetable oil (Lading et al., 1992).

In this present work, monoglyceride-based drug delivery systems were constructed in the ratio of 8:62:30 and 12:58:30 (triglyceride: monoglyceride: water). Two percent of mangostin extract was then incorporated into the samples. These ratios were chosen due to the water content of 30% gave the equilibrium water content and a separate water phase outside the liquid crystalline phase was not found. While the ratio of triglyceride between 8% and 12% resulted in the formation of the reversed hexagonal phases.

The differences in type and ratio of triglycerides were prepared to compare the effect of triglycerides on the physicochemical properties and *in vitro* drug release. The formulations used in this study are shown in Table 11. Formulations 1 to 3 and formulations 4 to 6 contained triglyceride: monoglyceride: water in the ratio of 8:62:30 and 12:58:30, respectively.

Table 11 Formulation of monoglyceride-based drug delivery system

Composition (% w/w)	Formulation					
	1	2	3	4	5	6
GMO	60.76	60.76	60.76	56.84	56.84	56.84
Sesame oil	7.84	-	-	11.76	-	-
Soybean oil	-	7.84	-	-	11.76	-
Olive oil	-	-	7.84	-	-	11.76
Water	29.40	29.40	29.40	29.40	29.40	29.40
Mangostin	2.00	2.00	2.00	2.00	2.00	2.00

E. Characterization of *Garcinia mangostana* Extract Monoglyceride-Based Drug Delivery System

1. Determination of Physicochemical Properties

The physicochemical properties of formulations before and after incorporating the *Garcinia mangostana* extract were determined as follows:

1.1 Physical Appearances

The physical appearances of formulations such as color, clarity and phase separation were observed. The color of monoglyceride-based drug delivery systems was light yellow, according to the color of glyceryl monooleate. After incorporation of mangostin extract, the color of formulations changed to dark yellow due to the deep yellow color of mangostin. The formulations before and after incorporation of mangostin extract were clear with some air bubbles due to the process of mixing, which disappeared when left to stand overnight. Phase separation and precipitation were not observed after incorporation of the mangostin extract. Different formulations showed the similar physical appearances.

1.2 pH Measurement

The pH of monoglyceride-based drug delivery systems before and after incorporation of mangostin extract was in the range of 5.42-5.60 and 5.68-5.84, respectively (Table 12). These results indicated that after incorporation of mangostin extract the pH values were slightly increased. The reason could not be clearly explained. Formulations 1 to 6 had the pH values in the same range.

Table 12 pH of formulation before and after incorporation of mangostin extract

Formulation	pH	
	Base	With mangostin
1	5.54±0.01	5.84±0.00
2	5.60±0.01	5.79±0.01
3	5.42±0.01	5.68±0.01
4	5.57±0.01	5.84±0.00
5	5.54±0.01	5.82±0.00
6	5.44±0.01	5.73±0.01

1.3 Viscosity Measurement

The viscosity values of monoglyceride-based drug delivery systems before and after incorporation of mangostin extract were in the range of 4758.94-5160.06 and 4824.34-5325.74 cps, respectively (Table 13). The viscosity of formulations with mangostin extract was slightly higher than that without the extract. The formulations with 8% triglyceride content (formulation 1-3) had higher viscosity than 12% triglyceride content (formulation 4-6). Analysis of data indicated that there was statistically significant difference between two groups ($P < 0.05$). However, all of the formulations are high-viscous enough to sustain release of drug at the injection sites.

Table 13 Viscosity of formulation before and after incorporation of mangostin extract

Formulation	Viscosity (cps)	
	Base	With mangostin
1	5160.06±49.38	5236.36±29.49
2	5140.44±23.58	5325.74±54.46
3	4979.12±46.40	5075.04±63.07
4	4874.48±29.49	4918.08±47.16
5	4826.52±17.30	4887.56±49.52
6	4758.94±22.97	4824.34±38.32

1.4 Polarized Light Microscopy

Photomicrographs of monoglyceride-based drug delivery systems before and after incorporation of mangostin extract are shown in Figures 37-38. The polarizing microscopic images showed similar pattern of liquid crystalline phases which indicated that mangostin extract did not affect the liquid crystal structure of the formulations. Different formulations also showed similar patterns of liquid crystalline phases.

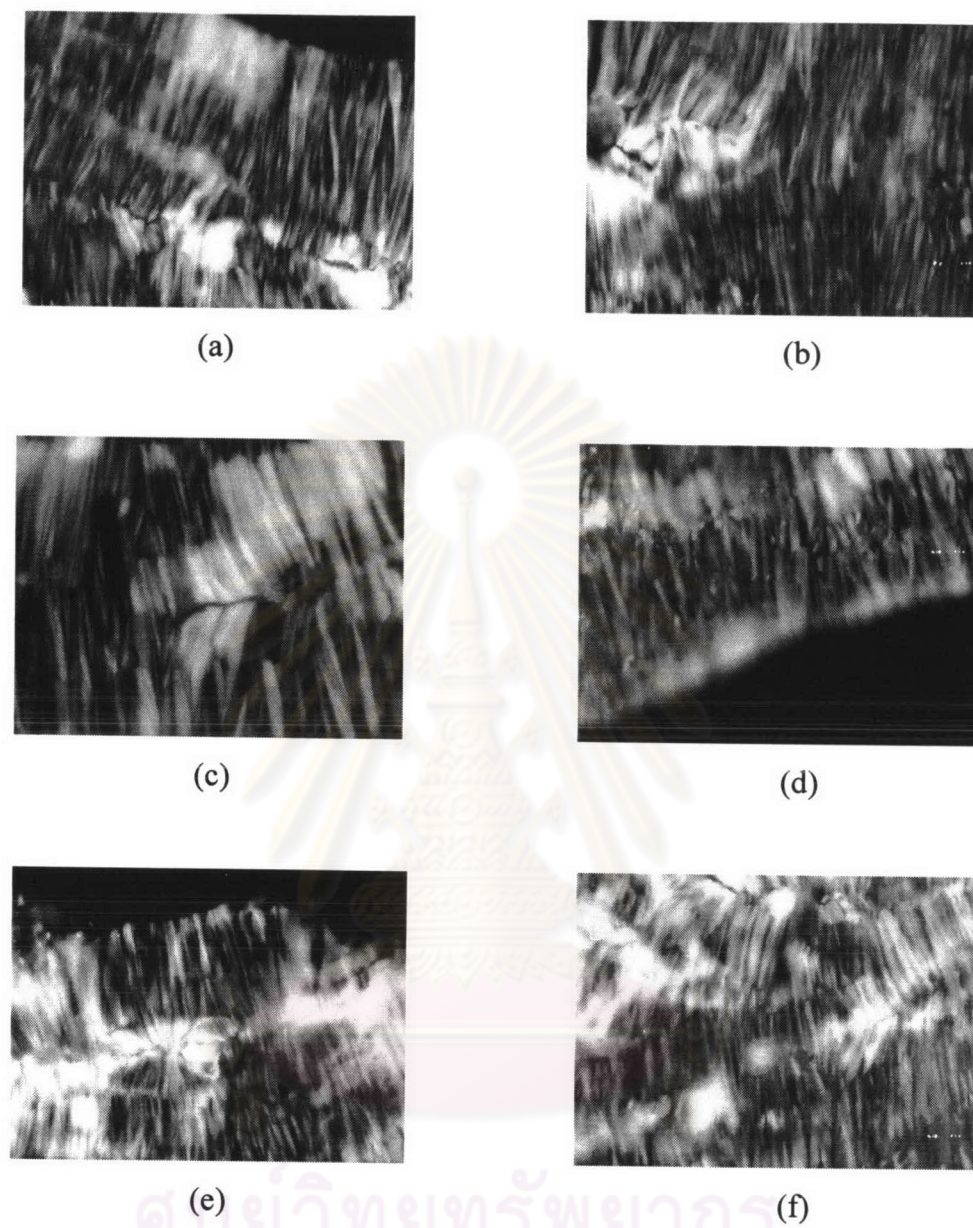


Figure 37 Polarizing microscopic images of formulation 1-3 before and after incorporation of mangostin extract; (a) and (b) formulation 1; (c) and (d) formulation 2; and (e) and (f) formulation 3, as observed at $\times 100$ magnification

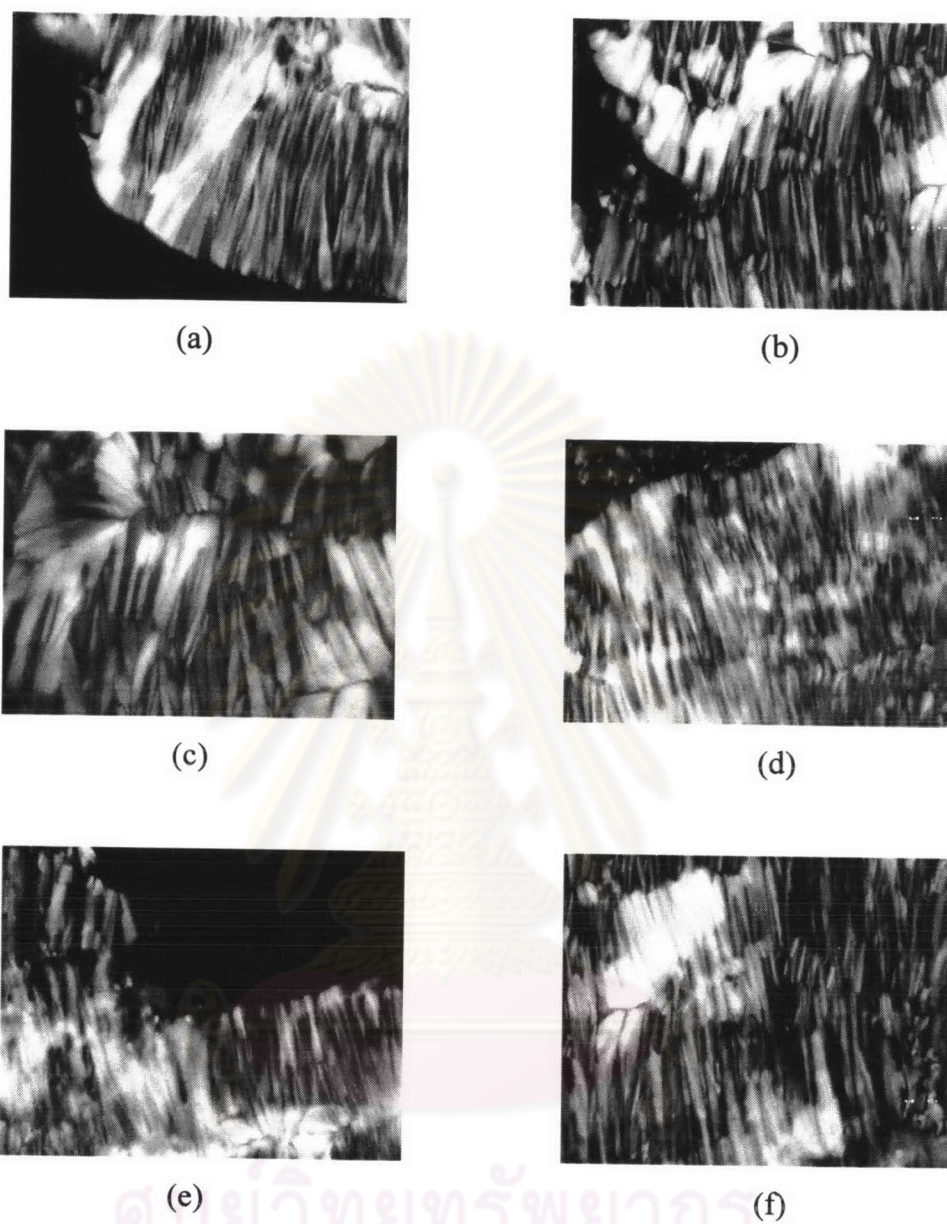


Figure 38 Polarizing microscopic images of formulation 4-6 before and after incorporation of mangostin extract; (a) and (b) formulation 4; (c) and (d) formulation 5; and (e) and (f) formulation 6, as observed at $\times 100$ magnification

2. Determination of Injectability through the Syringe

Due to their high viscosity and stiffness, liquid crystalline phases are difficult to administer through a syringe. Therefore, the low-viscous states are used and triggered to the high-viscous states by dilution with fluid in the oral cavity.

In this study, the injectability of low-viscous state formulations was determined by administer through the syringe with 23-gauge tip needle. The viscosity values of the formulations are shown in Table 14. Triglycerides have been reported to lower the melting point and improve the flow properties of glyceryl monooleate (Norling et al., 1992; Okonogi et al., 2004). As a result, the formulations with 12% triglyceride content could reduce the viscosity and improve the flow properties of the formulation more than 8% triglyceride content. Analysis of data indicated that there was statistically significant difference in the viscosity values between two groups ($P<0.05$). However, these viscosities were all low enough to be administered through the syringe with 23-gauge tip needle.

Table 14 Viscosity of low-viscous state formulation

Formulation	Viscosity (cps)
1	178.22±1.82
2	165.14±2.91
3	166.99±1.47
4	150.04±1.05
5	140.99±1.52
6	140.88±1.31

3. *In vitro* Liquid Crystalline Phase Formation Study

The *in situ* transition from a low-viscous state to the required high-viscous liquid crystalline phase after administration is important to the use of liquid crystalline phases for drug delivery. There are several parameters which may be used for triggering a transition *in situ* after administration. For glyceryl monooleate, the high-viscous liquid crystalline phases were formed upon contact with excess water.

This study was conducted with the low-viscous state formulations. After addition of the formulation into excess water, the liquid crystalline phase was detected by polarized light microscopy. As a result, all formulations could be transformed to the high-viscous liquid crystalline phase. The changes were found within 15 min after addition. Photographs from polarized light microscope showed the liquid crystals were formed and could be detected in 15 min (Figure 39). These results agreed with Scherlund et al. (2001), although there was a difference in liquid crystalline phase drug delivery system. Scherlund et al. suggested that in presence of a large amount of water, the samples take up the water immediately and form optically anisotropic phase, 30 min is enough to form the most of this phase.

The water uptake study of monoglyceride from Chang and Bodmeier (1997) showed that the water uptake initially increased rapidly and then leveled off and approached the equilibrium water content. The rapid swelling of the monoglyceride matrices indicated that the formation of the liquid crystalline phase was the fast process. These results were consistent with previous study. Geraghty et al. (1996) suggested that the rate of water uptake was inversely proportional to their initial water content. The hydration of monoglyceride containing 0% initial water content was observed within the first 15 min while the samples formulated with 40% water content did not hydrate or swell significantly as they already contained their equilibrium water content.

In conclusion, the *in vitro* study showed that low-viscous state formulations could be transformed to high-viscous liquid crystalline states upon dilution with water. Therefore it is possible to form this state after *in vivo* application.

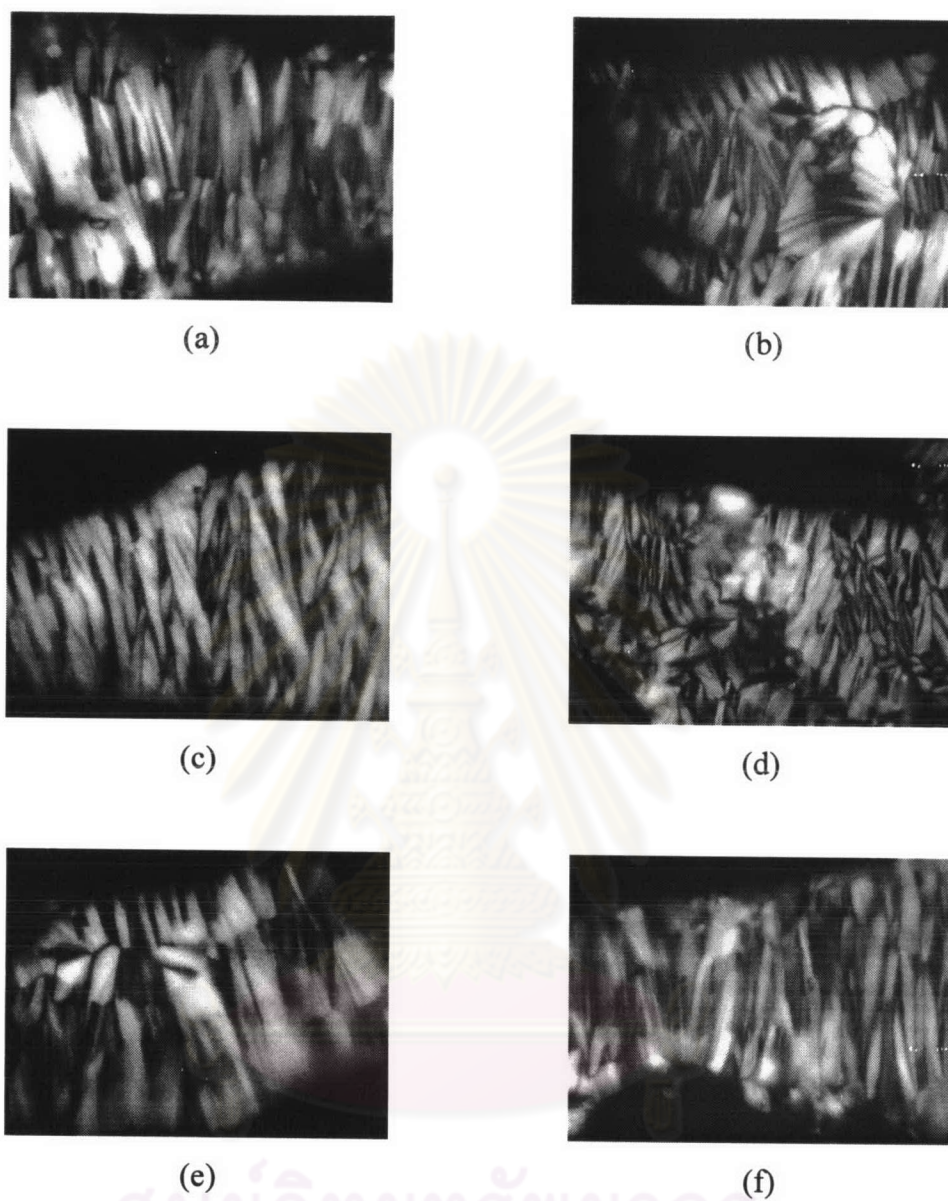


Figure 39 Polarizing microscopic images of *in vitro* liquid crystalline phase formation after dilution with water; (a) formulation 1; (b) formulation 2; (c) formulation 3; (d) formulation 4; (e) formulation 5; and (f) formulation 6, as observed at $\times 100$ magnification

4. *In Vitro* Release Study

4.1 Solubility Study of the Receiver Fluid

Although the pH of gingival crevice and periodontal pocket were reported in the mean of 6.92 ± 0.03 (Eggert et al., 1991), the most of *in vitro* release studies of drugs used in periodontal pocket used pH 7.4 phosphate buffer for the medium (Roskos et al., 1995; Esposito et al., 1996; Jones et al., 1997; Sendil et al., 1999; Schwach-Abdellaoui et al., 2001, 2002). Therefore, pH 7.4 phosphate buffer was used in this study. Because of the poor solubility of mangostin in this medium, ethanol was added into the medium to enhance drug solubility. In this present work, ethanol ranging from 0-35% was added into the receiver fluid and examined the solubility of mangostin. The results showed that the solubility of mangostin was increased as a function of ethanol concentrations (Table 15). The solubility of mangostin in pH 7.4 phosphate buffer was 0.0234 ± 0.0030 mg/ml and in the present of 35% ethanol the solubility was increased to 1.1277 ± 0.0886 mg/ml, which was able to maintain the sink condition in the release study.

Table 15 Solubility of mangostin in pH 7.4 phosphate buffer and various concentrations of ethanol in pH 7.4 phosphate buffer

Solvent	Solubility (mg/ml)
pH 7.4 phosphate buffer	0.0234 ± 0.0030
pH 7.4 phosphate buffer+10% ethanol	0.0559 ± 0.0047
pH 7.4 phosphate buffer+20% ethanol	0.1008 ± 0.0109
pH 7.4 phosphate buffer+25% ethanol	0.1965 ± 0.0230
pH 7.4 phosphate buffer+30% ethanol	0.4550 ± 0.0568
pH 7.4 phosphate buffer+35% ethanol	1.1277 ± 0.0886

4.2 *In vitro* Release Study

In vitro drug release methods are frequently used to gain information about the release profiles of active ingredients in the formulation development. In the present work, two compartment Franz diffusion cells were used for the experiments. The amounts of drug release were analyzed using UV spectrophotometer. The validation methods are shown in the following part.

The release profiles were plotted between the cumulative amounts of drug release versus time as shown in Figures 40-41. The release data are presented in Appendix B. All formulations could sustain the release of drug over a period of 48 hr. These results were consistent with previous reports. Norling et al. (1992) reported that the reversed hexagonal form of monoglyceride-based drug delivery system could give a sustained release of drug over a period of 48 hr while the cubic form showed a complete release in 24 hr. Because of the diffusion pathway is more obstructed in the reversed hexagonal form than in the cubic one, which has connected water channels. The closed water channels of the reversed hexagonal phase slow down the diffusion of dissolved drug through the matrix. *In vivo* results from Esposito et al. (1996) showed that monoglyceride-based drug delivery system was persistent in the periodontal pockets with 80% of the initial level after 8 hr of application.

In the present study, various oils showed similar release profiles but there was a slight difference in the percentages of drug release. The highest drug release was obtained from the formulations with sesame oil, followed by soybean oil and olive oil, respectively. However, analysis of data indicated that there was no statistically significant difference ($P>0.05$) in overall percentages of drug release. The formulations with 8% triglycerides content showed less percentage of drug release at the beginning of the release profiles than the formulations with 12% triglycerides content but overall percentages of drug release were similar in the range of 91.97-94.46%. In addition, the formulations with 8% triglycerides content did not show more prolonged release over a period of study. These data indicated that increasing triglycerides content of the formulations could improve the flow properties and injectability of the formulation into the periodontal pockets but did not affect the release-controlling mechanism of the drug delivery system.

Several mathematical models have been used to describe the release of the drug. The release data obtained from this study were plotted according to the following models to describe the mechanism of drug release: zero-order kinetics, first-order kinetics, and Higuchi diffusion model where the cumulative amount of drug release per unit surface area is directly proportional to the square root of time.

$$\text{Zero-order equation: } Q_t = Q_0 - k_0t$$

$$\text{First order equation: } \ln Q_t = \ln Q_0 - k_1t$$

$$\text{Higuchi's equation: } Q_t = k_H t^{1/2}$$

where Q_t is the amount of drug release at time t , k_0 is the zero-order release rate constant, k_1 is the first-order release rate constant, and k_H is the diffusion rate constant.

The kinetic parameters for zero-order, first-order and Higuchi model during the initial 24 hr were calculated and are presented in Table 16. The zero-order plot, the first-order plot and the Higuchi plot are shown in Figures 40-41, Figures 42-43 and Figures 44-45, respectively. The release data of mangostin tend to follow Higuchi model rather than the other two models, because the highest coefficient of determination (R^2) was obtained with the Higuchi model. Analysis of data showed that there was statistically significant difference ($P < 0.05$) in coefficients of determination between the three models. Moreover, analysis of variance by regression showed a significant difference ($P < 0.05$) in coefficients of determination of the Higuchi model, which indicated the correlation of % cumulative release and square root of time. The highest Higuchi release rate constant was obtained from the formulations with olive oil. Analysis of data indicated that the Higuchi release rate constant of the formulations with olive oil was statistically significant difference ($P < 0.05$) than the formulations with sesame oil and soybean oil but there was no statistically significant difference ($P > 0.05$) in the release rate constant between the formulations with sesame oil and soybean oil.

The mechanism of diffusion controlled release (Higuchi, 1961, 1963) was dominated by the penetration of the medium into the drug matrix through the channels of the liquid crystalline phase, and then the drug was presumed to leach out by gradually dissolving into the permeating medium and diffusing from the matrix along the channels filled with the extracting medium. Thus, the release behavior of drug was expected to be governed by the solubility and diffusion coefficient of the drug in the liquid crystalline phase. This mechanism was explained by Higuchi's equation as follows:

$$Q = \frac{[D\varepsilon (2A - \varepsilon C_s) C_s t]^{1/2}}{\tau}$$

where Q is the amount of drug release after time t per unit exposed area, D is the diffusion coefficient of the drug in the matrix, ε is the porosity of the matrix, τ is the tortuosity factor of the matrix, A is the total amount of drug in the matrix per unit volume, and C_s is the solubility of drug in the matrix.

The result from this study conformed to many reports which suggested that the release mechanism from monoglyceride-based drug delivery system followed square root of time kinetics indicating that the rate of release was diffusion controlled (Geraghty et al., 1996; Chang and Bodmeier, 1997; Komsri, 1997; Helledi and Schubert, 2001). However, other studies showed that monoglyceride-based drug delivery system could be followed zero-order and first-order kinetics (Burrows, Collett and Attwood, 1994). These data indicated that the similar liquid crystalline system could demonstrate different release profiles. These depend on several factors including a wide range of drug, solubility and concentration of the incorporated drug substance.

Table 16 Kinetic parameters of mangostin release from monoglyceride-based drug delivery system

Formulation	Zero-order plot		First-order plot		Higuchi plot	
	k_0	R^2	k_1	R^2	k_H	R^2
1	2.5407	0.8806	0.0488	0.7528	16.1968	0.9791
2	2.6269	0.8845	0.0541	0.7572	16.6843	0.9761
3	2.8727	0.8570	0.0667	0.6816	18.4496	0.9671
4	2.6607	0.9046	0.0473	0.7977	16.7773	0.9840
5	2.7437	0.9068	0.0504	0.7908	17.2936	0.9856
6	3.0679	0.8834	0.0647	0.7337	19.4843	0.9748

ศูนย์วิทยทรัพยากร
จุฬาลงกรณ์มหาวิทยาลัย

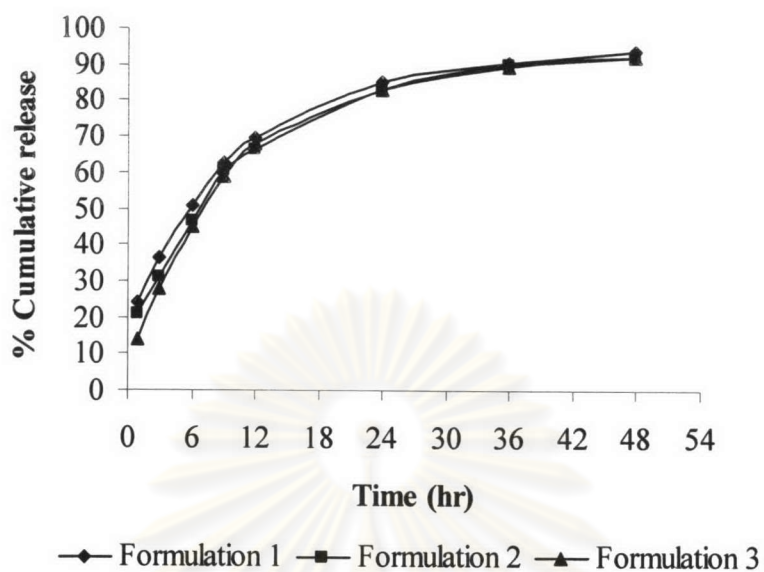


Figure 40 Release profiles of mangostin from monoglyceride-based drug delivery system containing triglyceride: monoglyceride: water in the ratio of 8:62:30

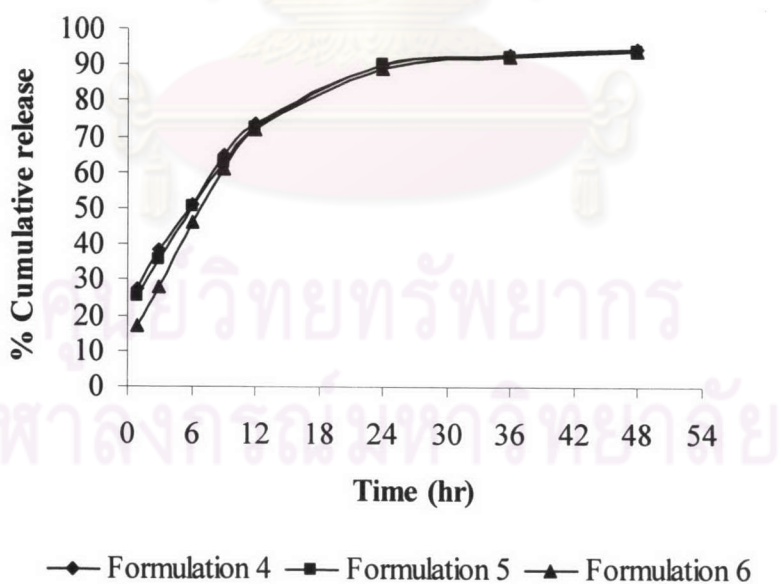


Figure 41 Release profiles of mangostin from monoglyceride-based drug delivery system containing triglyceride: monoglyceride: water in the ratio of 12:58:30

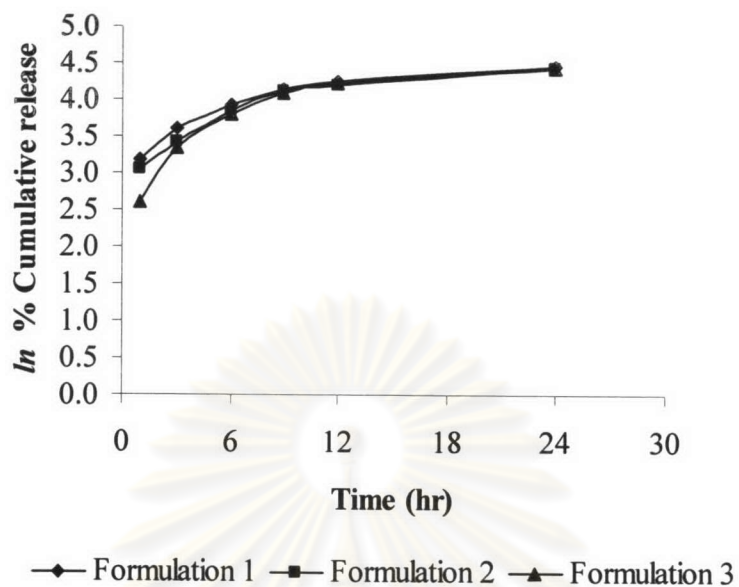


Figure 42 First-order plot of mangostin from monoglyceride-based drug delivery system containing triglyceride: monoglyceride: water in the ratio of 8:62:30

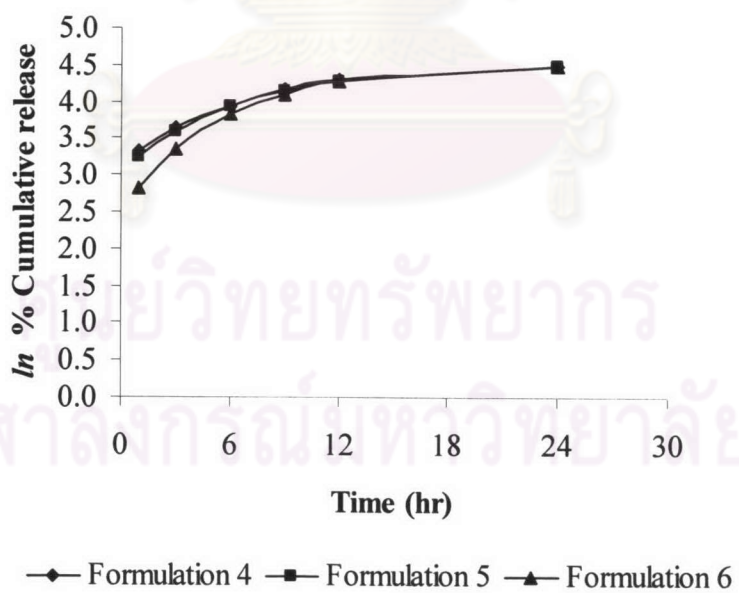


Figure 43 First-order plot of mangostin from monoglyceride-based drug delivery system containing triglyceride: monoglyceride: water in the ratio of 12:58:30

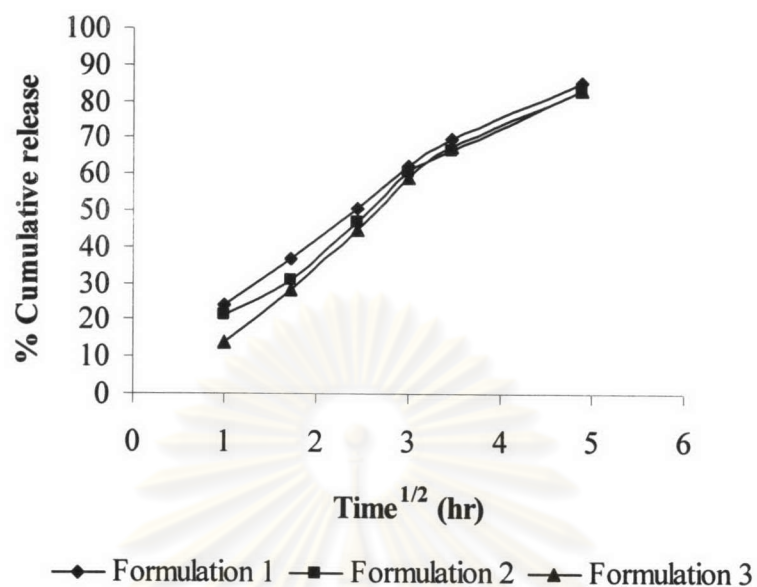


Figure 44 Higuchi plot of mangostin from monoglyceride-based drug delivery system containing triglyceride: monoglyceride: water in the ratio of 8:62:30

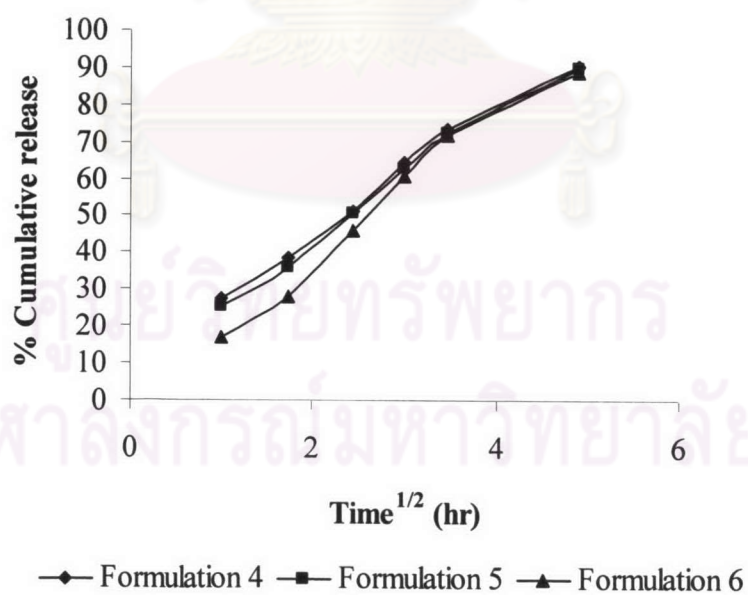


Figure 45 Higuchi plot of mangostin from monoglyceride-based drug delivery system containing triglyceride: monoglyceride: water in the ratio of 12:58:30

4.3 Validation of UV Spectrophotometric Method

The validation of analytical method is the process for evaluation that the method is suitable and reliable for the intended analytical applications. The analytical parameters used for the UV spectrophotometric assay validation were specificity, linearity, accuracy and precision.

4.3.1 Specificity

The UV absorption spectrum of mangostin is shown in Figure 46. The maximum absorbance was found at the wavelength of 243 nm. Therefore, the detection of mangostin was performed at this wavelength. Furthermore, under the condition selected for *in vitro* release study, the peak of other components in the formulations was not interfering with the peak of mangostin (Figure 47). This validation was made by comparing the peak scan from UV spectrophotometer between the receptor fluids taken at 48 hr from the formulations without incorporated mangostin with the peak of mangostin.

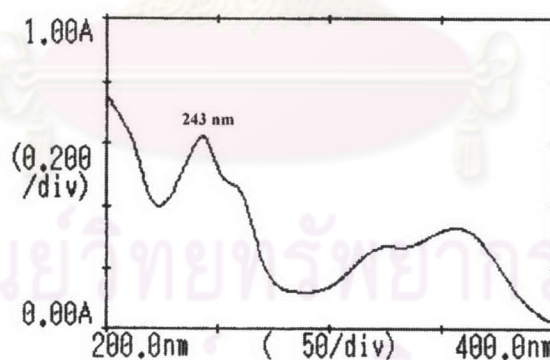
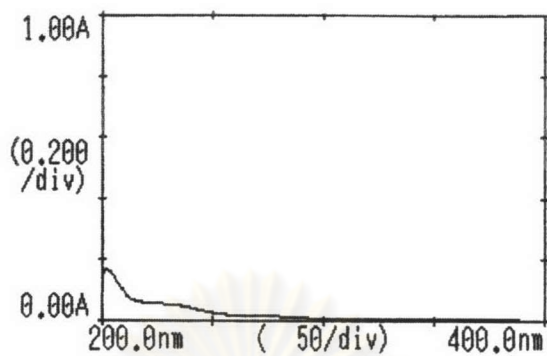
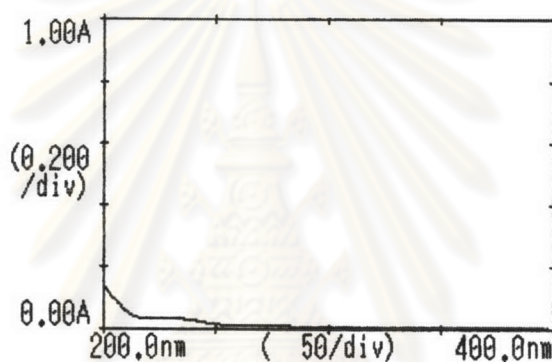


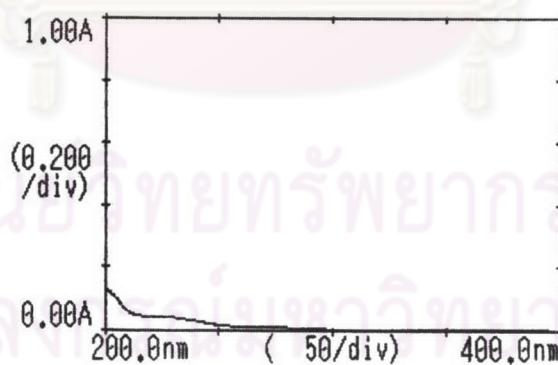
Figure 46 UV spectrum of mangostin in 35% ethanol in pH 7.4 phosphate buffer



(a)



(b)



(c)

Figure 47 UV spectra of the receptor fluid taken from non-drug formulations; (a) sample with sesame oil; (b) sample with soybean oil; and (c) sample with olive oil

4.3.2 Linearity

The calibration curve of mangostin in 35% ethanol in pH 7.4 phosphate buffer was shown in Figure 48. Linear regression analysis of the absorbances versus the corresponding concentrations was performed and the coefficient of determination (R^2) was calculated as 0.9999. The calibration data were found to be linear with excellent coefficient of determination. These results indicated that UV spectrophotometric method was acceptable for quantitative analysis of mangostin in the range studied.

Table 17 Data for calibration curve of mangostin by UV spectrophotometric method

Concentration ($\mu\text{g/ml}$)	Absorbance			Mean	SD	%CV
	Set 1	Set 2	Set 3			
2.40	0.206	0.204	0.205	0.205	0.001	0.49
3.60	0.312	0.315	0.311	0.313	0.002	0.67
4.80	0.420	0.420	0.424	0.421	0.002	0.55
6.00	0.529	0.532	0.528	0.530	0.002	0.39
7.20	0.632	0.633	0.634	0.633	0.001	0.16
8.40	0.743	0.739	0.740	0.741	0.002	0.28
9.60	0.844	0.848	0.844	0.845	0.002	0.27
R^2	0.9999	0.9999	0.9999	0.9999	-	-

ศูนย์วิทยทรัพยากร
จุฬาลงกรณ์มหาวิทยาลัย

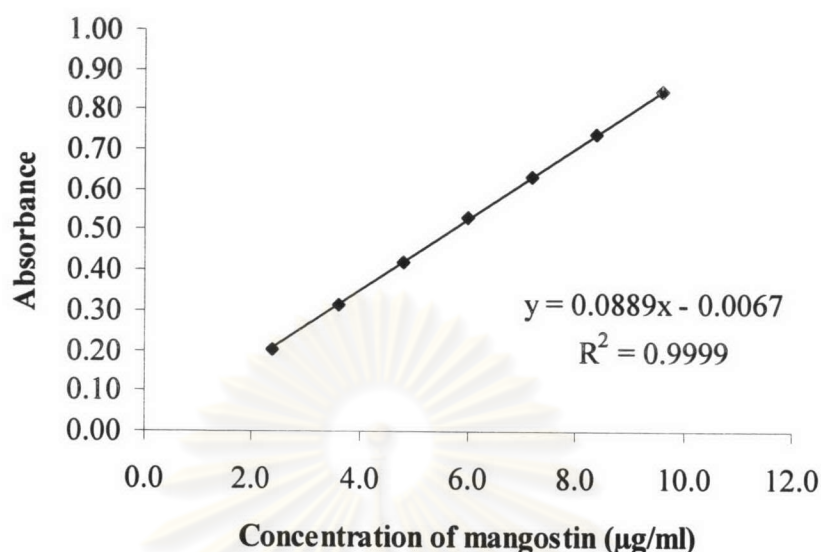


Figure 48 Calibration curve of mangostin by UV spectrophotometric method

4.3.3 Accuracy

Mangostin solutions were prepared at the concentration of 2.40, 6.00, and 9.60 µg/ml in five sets. Each individual sample was analyzed by UV spectrophotometer. The inversely estimated concentrations and percentages of analytical recovery of each drug concentration are shown in Table 18 and Table 19, respectively. All percentages of analytical recovery were in the range of 99.02-100.19%, which indicated the high accuracy of this method. Thus, it could be used for analysis of mangostin in all concentrations studied.

Table 18 The inversely estimated concentrations of mangostin by UV spectrophotometric method

Concentration (µg/ml)	Inversely estimated concentration (µg/ml)					Mean ± SD
	Set 1	Set 2	Set 3	Set 4	Set 5	
2.40	2.3583	2.4150	2.3697	2.3583	2.3810	2.3764±0.02
6.00	6.0048	6.0728	5.9822	5.9709	6.0275	6.0116±0.04
9.60	9.5607	9.5834	9.6513	9.5154	9.5720	9.5766±0.05

Table 19 The percentage of analytical recovery of mangostin by UV spectrophotometric method

Concentration ($\mu\text{g/ml}$)	% Analytical recovery					Mean \pm SD
	Set 1	Set 2	Set 3	Set 4	Set 5	
2.40	98.26	100.62	98.74	98.26	99.21	99.02 \pm 0.98
6.00	100.08	101.21	99.70	99.51	100.46	100.19 \pm 0.68
9.60	99.59	99.83	100.53	99.12	99.71	99.76 \pm 0.51

4.3.4 Precision

The precision of mangostin analyzed by UV spectrophotometric method were determined both within run precision and between run precision as illustrated in Tables 20-21. All coefficient of variation values were very low, as 0.52-1.01% and 0.76-1.24%, respectively. The coefficient of variation of an analytical method should generally be less than 2%. Therefore, the UV spectrophotometric method was precise for quantitative analysis of mangostin in the range studied.

Table 20 Data of within run precision by UV spectrophotometric method

Concentration ($\mu\text{g/ml}$)	Absorbance					Mean	SD	%CV
	Set 1	Set 2	Set 3	Set 4	Set 5			
2.40	0.203	0.208	0.204	0.203	0.205	0.205	0.002	1.01
6.00	0.525	0.531	0.523	0.522	0.527	0.526	0.003	0.68
9.60	0.839	0.847	0.841	0.835	0.840	0.840	0.004	0.52

Table 21 Data of between run precision by UV spectrophotometric method

Concentration ($\mu\text{g/ml}$)	Absorbance					Mean	SD	%CV
	Set 1	Set 2	Set 3	Set 4	Set 5			
2.40	0.204	0.199	0.201	0.205	0.204	0.203	0.002	1.24
6.00	0.523	0.517	0.525	0.530	0.522	0.523	0.004	0.90
9.60	0.848	0.831	0.841	0.845	0.842	0.841	0.006	0.76

In conclusion, the analysis of mangostin in 35% ethanol in pH 7.4 phosphate buffer by UV spectrophotometric method developed in this study showed good specificity, linearity, accuracy and precision. Thus this method was used for the determination of the content of mangostin in the *in vitro* release study.

5. Differential Scanning Calorimetric (DSC) Method

DSC is a thermal analysis method for detecting changes in physical or chemical properties of materials as a function of temperature. The hydrocarbon chains of amphiphilic molecules are subjected to undergoing a transformation from an order (gel) state to a more disorder (liquid crystalline) state. These changes have been characterized by DSC which requires the input of additional thermal energy show up as endothermic peaks on heating.

In the temperature range of -20 to 60 °C, DSC thermograms of liquid crystalline state showed broad endothermic peaks at temperature range of -10 to 0 °C (Figures 50-51). Both samples with and without mangostin showed similarly in pattern of the peaks and temperature range. No other endothermic peak was observed within the studied temperature range. The presence of these peaks was possible that a phase transition occurred. In this study, DSC thermograms presented two endothermic peaks which might be correspond to the gel to liquid crystal transition and the pretransition peaks, which was due to a rearrangement of the molecules in the structure (Koyama et al., 1999). Chang and Bodmeier (1996) reported that the phase transitions of glyceryl monooleate-water mixtures were below room temperature. This suggested that the liquid crystalline phase should remain physically stable in the studied temperature range without phase transformation. Therefore, they could be stored at room temperature. In addition, the study showed the transition temperature decreased from 25 °C to 7 °C when the water content increased from 0% to 30%. Helledi and Schubert (2001) reported that no phase transition of the liquid crystalline phase from glyceryl monooleate was detected in the temperature range of 20 to 70 °C both samples with and without addition of drug. These results demonstrated that the

drug can be incorporated into the liquid crystalline phase without causing phase transition.

In the temperature range of -20 to 250 °C, the DSC thermograms of liquid crystalline state both formulations with and without mangostin showed endothermic peaks at temperature range of 123.94 to 133.45 °C (Figures 52-57), while the DSC thermogram of pure compounds used in this study (Figure 49) did not present the peaks in that temperature range. The presence of these peaks was possible that the water was desolvated from the bound water in liquid crystalline state. In the samples containing mangostin, the melting peak of mangostin in the temperature range of 179 to 180 °C as described in Figure 23 was not found. The possible explanation is that mangostin was incorporated into the liquid crystal structures and could not be detected.

In conclusion, the liquid crystalline phase remained physically stable in the studied temperature range without phase transformation. In addition, mangostin does not influence the transition behavior and can be incorporated into the liquid crystalline phase without causing phase transition.



ศูนย์วิทยทรัพยากร
จุฬาลงกรณ์มหาวิทยาลัย

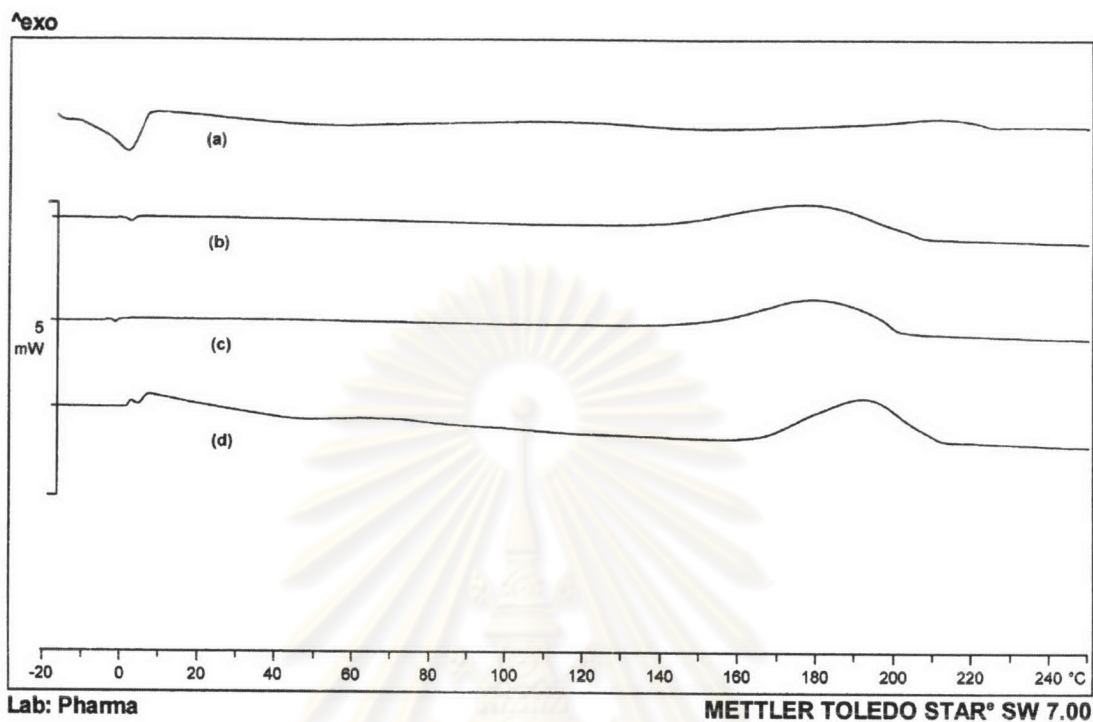


Figure 49 DSC thermogram of pure compounds in the temperature range of -20 to 250 °C; (a) glyceryl monooleate (sample weight 4.36 mg); (b) sesame oil (sample weight 3.76 mg); (c) soybean oil (sample weight 3.34 mg); and (d) olive oil (sample weight 3.58 mg)

ศูนย์วิทยทรัพยากร
จุฬาลงกรณ์มหาวิทยาลัย

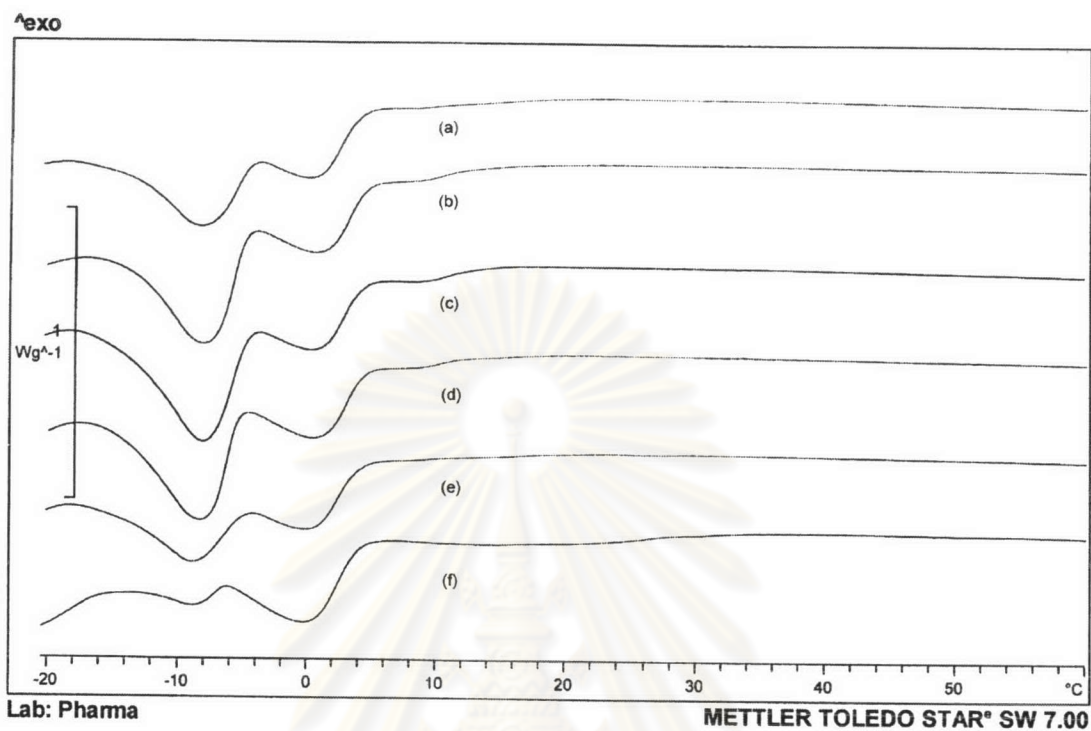


Figure 50 DSC thermogram of formulation 1-3 in the temperature range of -20 to 60 °C; (a) formulation 1 with mangostin (sample weight 4.00 mg); (b) formulation 1 without mangostin (sample weight 4.04 mg); (c) formulation 2 with mangostin (sample weight 4.12 mg); (d) formulation 2 without mangostin (sample weight 4.11 mg); (e) formulation 3 with mangostin (sample weight 4.08 mg); and (f) formulation 3 without mangostin (sample weight 4.20 mg)

ศูนย์วิทยทรัพยากร
จุฬาลงกรณ์มหาวิทยาลัย

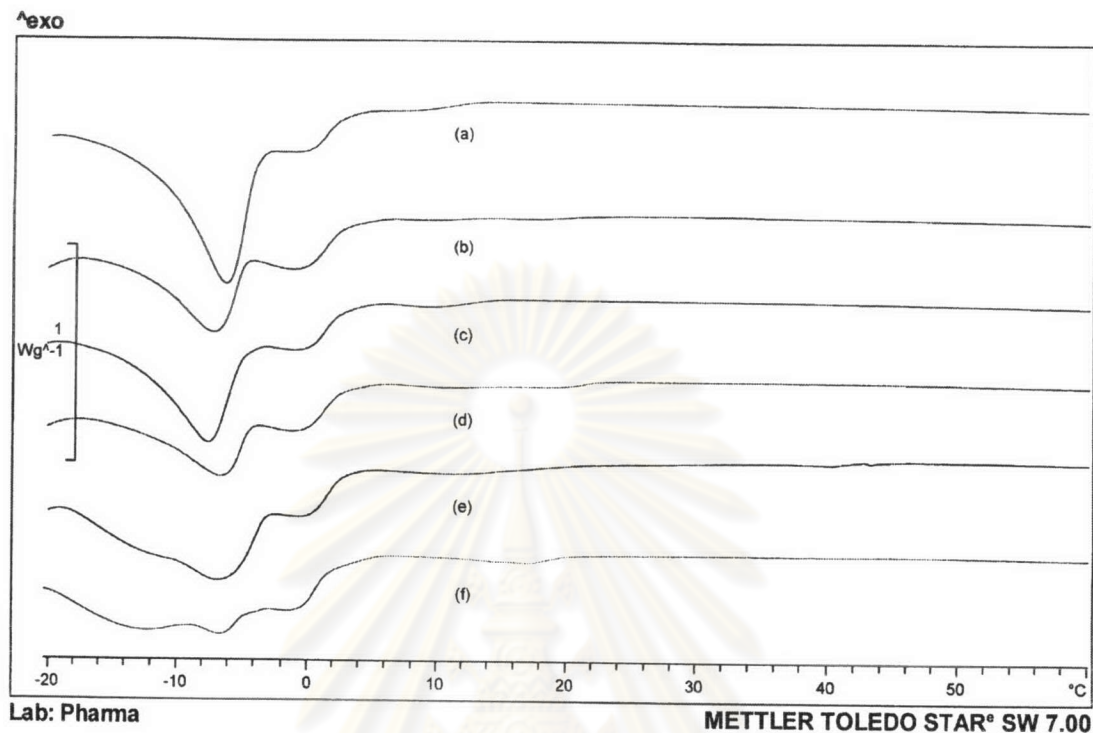


Figure 51 DSC thermogram of formulation 4-6 in the temperature range of -20 to 60 °C; (a) formulation 4 with mangostin (sample weight 4.04 mg); (b) formulation 4 without mangostin (sample weight 4.03 mg); (c) formulation 5 with mangostin (sample weight 4.17 mg); (d) formulation 5 without mangostin (sample weight 4.12 mg); (e) formulation 6 with mangostin (sample weight 4.07 mg); and (f) formulation 6 without mangostin (sample weight 4.08 mg)

ศูนย์วิจัยทรัพยากร
จุฬาลงกรณ์มหาวิทยาลัย

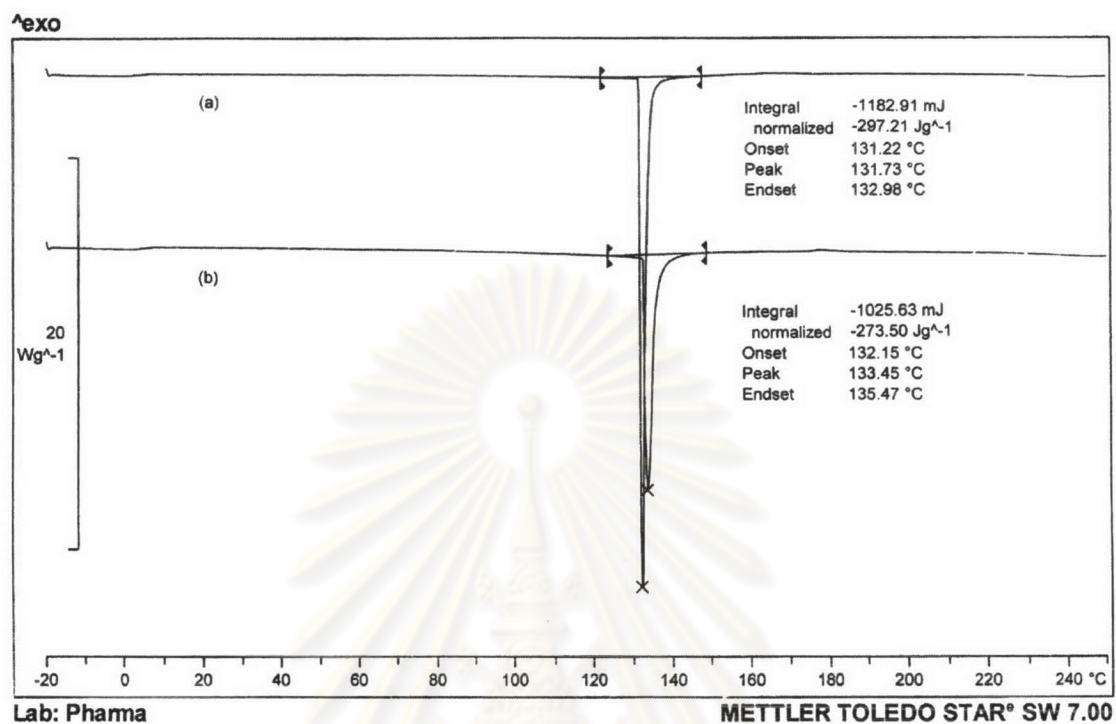


Figure 52 DSC thermogram of formulation 1 in the temperature range of -20 to 250 °C; (a) formulation 1 with mangostin (sample weight 4.00 mg); and (b) formulation 1 without mangostin (sample weight 4.03 mg)

ศูนย์วิทยทรัพยากร
จุฬาลงกรณ์มหาวิทยาลัย

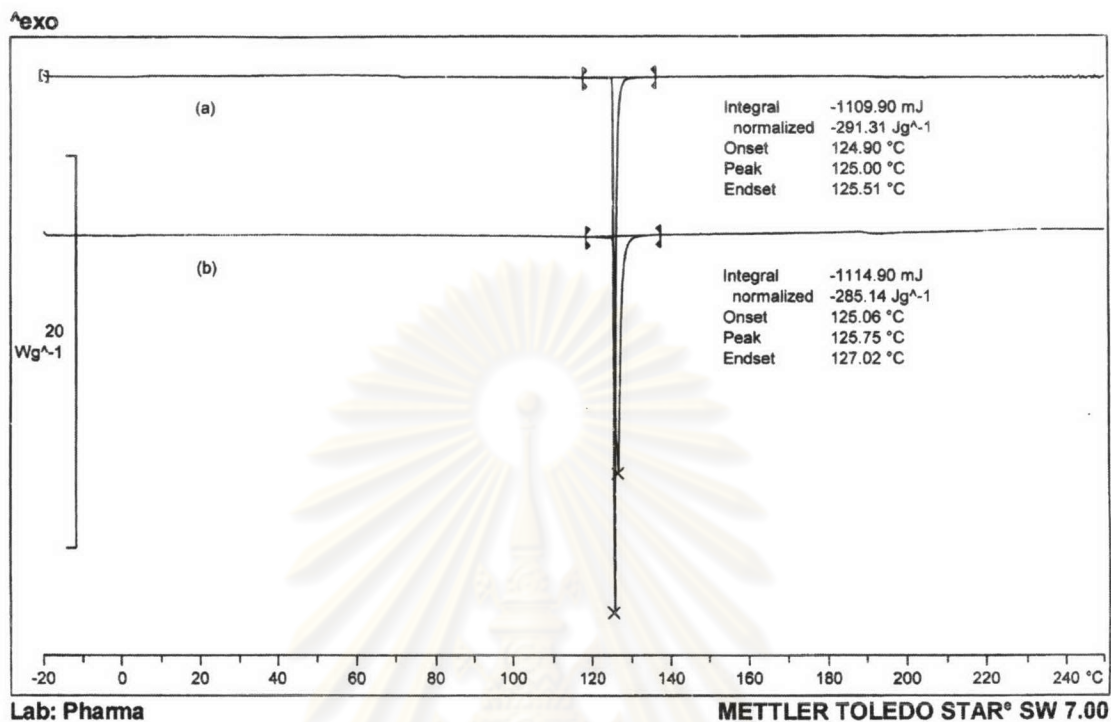


Figure 53 DSC thermogram of formulation 2 in the temperature range of -20 to 250 °C; (a) formulation 2 with mangostin (sample weight 3.81 mg); and (b) formulation 2 without mangostin (sample weight 3.91 mg)

ศูนย์วิทยทรัพยากร
จุฬาลงกรณ์มหาวิทยาลัย

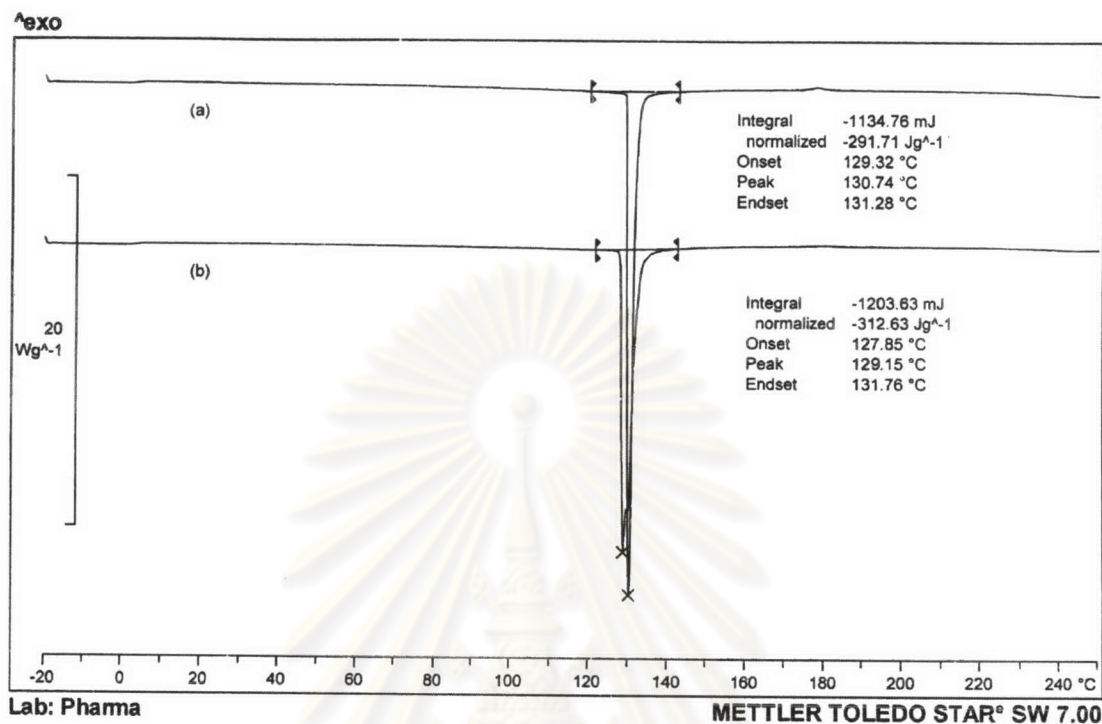


Figure 54 DSC thermogram of formulation 3 in the temperature range of -20 to 250 °C; (a) formulation 3 with mangostin (sample weight 3.89 mg); and (b) formulation 3 without mangostin (sample weight 3.85 mg)

ศูนย์วิทยทรัพยากร
จุฬาลงกรณ์มหาวิทยาลัย

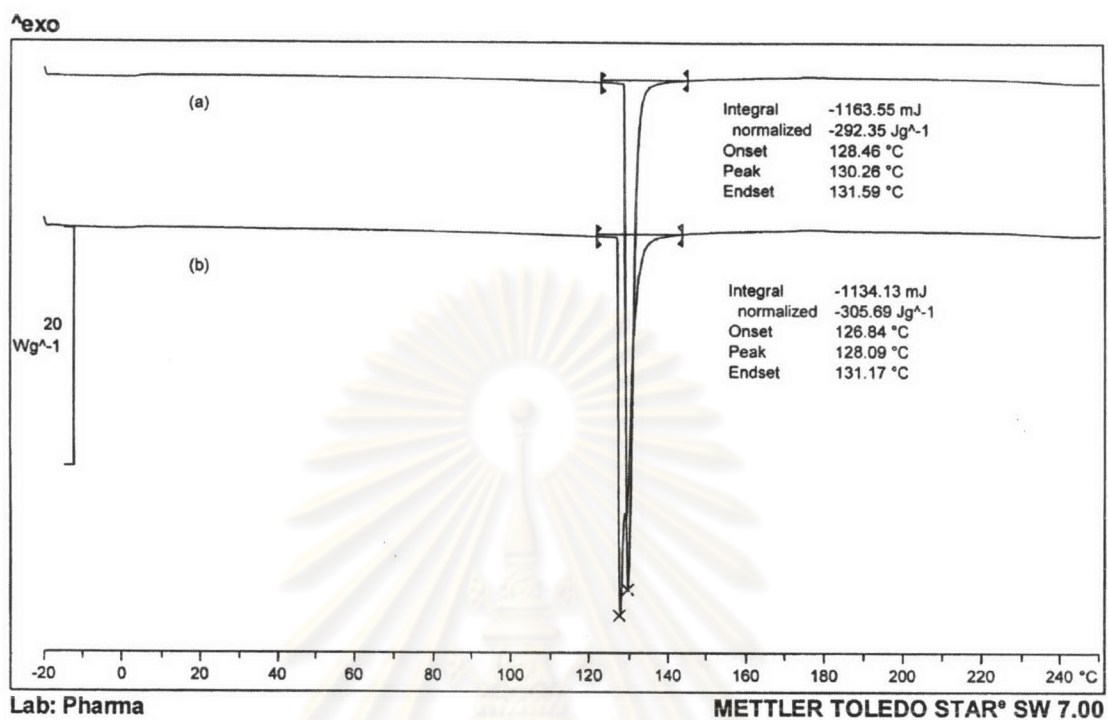


Figure 55 DSC thermogram of formulation 4 in the temperature range of -20 to 250 °C; (a) formulation 4 with mangostin (sample weight 3.71 mg); and (b) formulation 4 without mangostin (sample weight 3.98 mg)

ศูนย์วิทยทรัพยากร
จุฬาลงกรณ์มหาวิทยาลัย

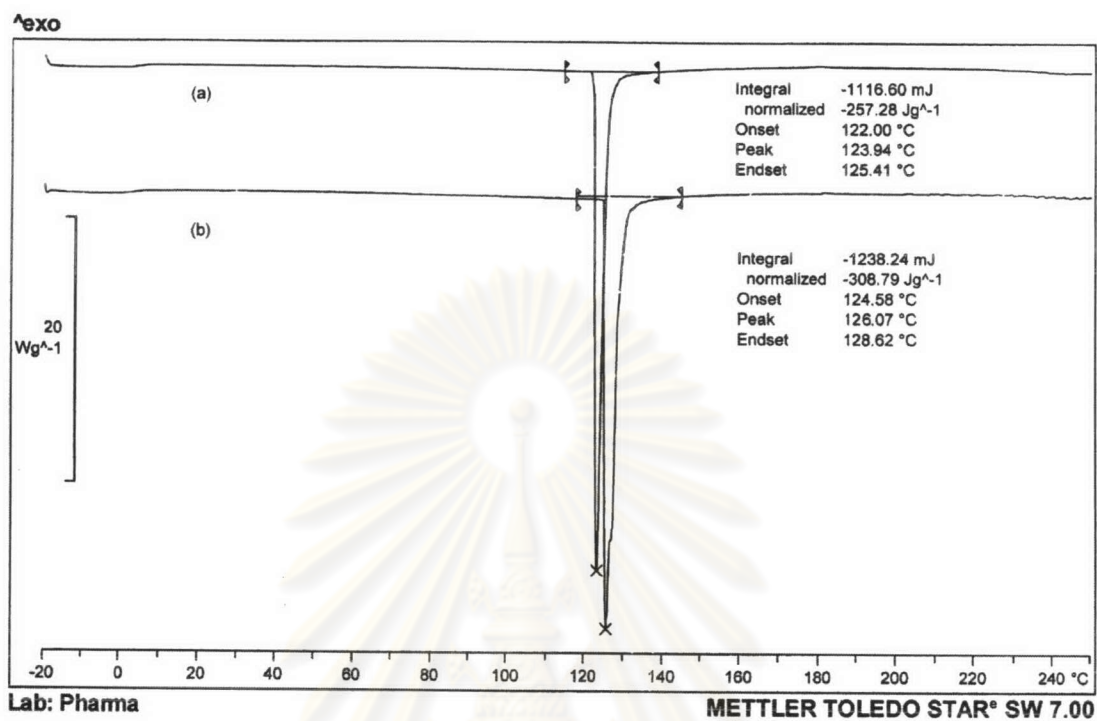


Figure 56 DSC thermogram of formulation 5 in the temperature range of -20 to 250 °C; (a) formulation 5 with mangostin (sample weight 3.90 mg); and (b) formulation 5 without mangostin (sample weight 4.01 mg)

ศูนย์วิทยทรัพยากร
จุฬาลงกรณ์มหาวิทยาลัย

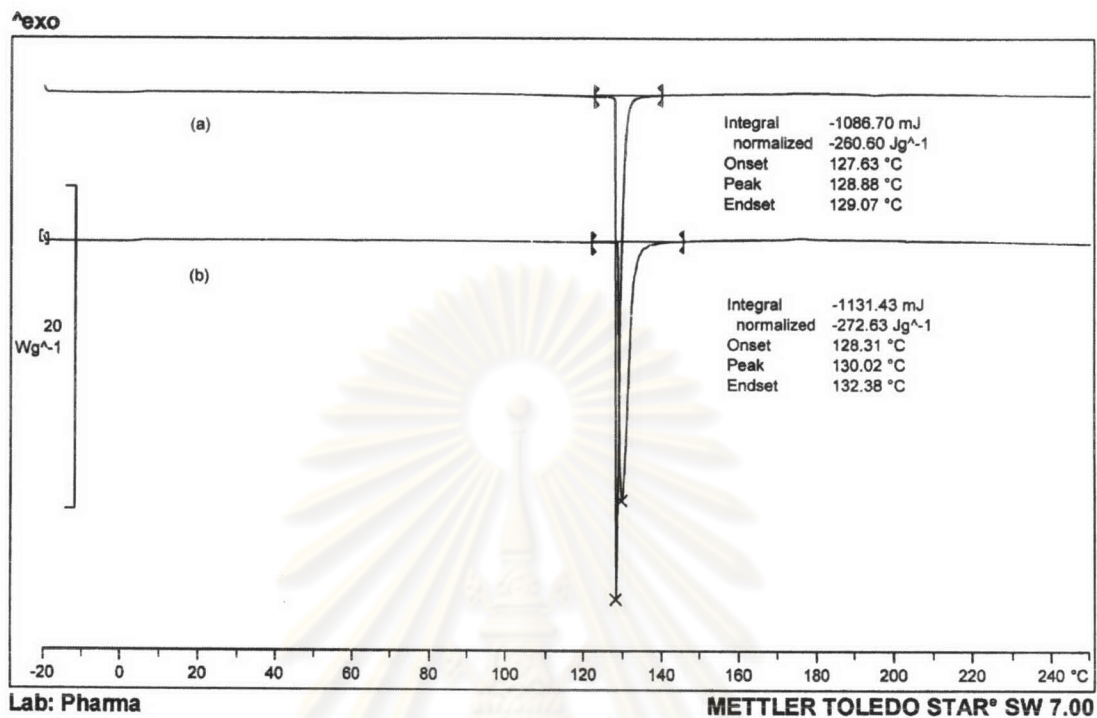


Figure 57 DSC thermogram of formulation 6 in the temperature range of -20 to 250 °C; (a) formulation 6 with mangostin (sample weight 4.17 mg); and (b) formulation 6 without mangostin (sample weight 4.15 mg)

ศูนย์วิทยทรัพยากร
จุฬาลงกรณ์มหาวิทยาลัย

6. Determination of Antimicrobial Activity of *Garcinia mangostana* Extract Monoglyceride-Based Drug Delivery System

It is well documented that dental caries and the progression to periodontal diseases begin with an accumulation of bacteria in dental plaque. The main microorganism linked with dental plaque seems to be *Streptococcus mutans*.

From previous unpublished data performed by Torrungruang, K., and Vichienroj, P., Department of Periodontology, Faculty of Dentistry, Chulalongkorn University, it was found that *Garcinia mangostana* extract derived from this study exhibited antimicrobial activity against *Streptococcus mutans* KPSK₂ and *Porphyromonas gingivalis* W50, the microbial species associated with dental caries and periodontal diseases, respectively. The minimum inhibitory concentration (MIC) and minimum bactericidal concentration (MBC) of *Streptococcus mutans* KPSK₂ and *Porphyromonas gingivalis* W50 are shown in Table 22.

Table 22 MIC and MBC of *Garcinia mangostana* extract on *Streptococcus mutans* KPSK₂ and *Porphyromonas gingivalis* W50

Types of bacteria	MIC (µg/ml)	MBC (µg/ml)
<i>Streptococcus mutans</i> KPSK ₂	0.625	1.250
<i>Porphyromonas gingivalis</i> W50	20	40

The agar diffusion method is the method for determining the antimicrobial susceptibility pattern of a bacterial strain. A filter paper disk, a hole, a porous cup or an open-ended cylinder containing measured quantities of drug is placed on a solid medium that has been heavily seeded with the test organisms. In this study, the antimicrobial activity against *Streptococcus mutans* KPSK₂ was examined by using a hole for placed the samples. When bacterial multiplication proceeds more rapidly than the drug can diffuse, the bacterial cells that are not inhibited by the antimicrobial will continue to multiply until a lawn of growth is visible and no zone of inhibition appears around the hole. When the antimicrobial is present in inhibitory concentrations, no growth will appear in the zone around the hole.

As a result, all formulations with and without mangostin showed no inhibition zone. The result obtained was quite unexpected. The question was whether mangostin extract had lost the antimicrobial activity or mangostin extract could not release from the formulation. Therefore, mangostin extract was tested for antimicrobial activity against *Streptococcus mutans* KPSK₂ by agar diffusion method using the same condition. Two percent of mangostin extract in 95% ethanol, equivalent to the formulations, was used in this study. The result showed that mangostin had an inhibition zone with a diameter of 15.33 ± 0.29 mm, which indicated that mangostin had an antimicrobial activity against *Streptococcus mutans* KPSK₂. From visual inspection, all formulations with and without mangostin could not diffuse into the surrounding medium, they still contained in the hole. In contrast, mangostin extract in 95% ethanol diffused into the medium and presented an empty hole with inhibition zone. The probable explanation is that these formulations are oily semi-solid, which is immiscible to aqueous solid medium. Since, mangostin extract is lipophilicity (from the following study) therefore it likes the more lipophilic region and does not diffuse into the medium. To solve this problem, the formulation with more hydrophilicity should be prepared. Increasing the water content in the formulation can increase the hydrophilicity. However, the result from the previous study indicated that the higher water content than 30% could not make the high-viscous liquid crystalline phase, it appears to be two-phase separation. Therefore, another aqueous formulation preparing from poloxamer 407 was used in this study.

Poloxamer 407 is a series of closely related block copolymers of ethylene oxide and propylene oxide. Poloxamer 407 displays a temperature-induced thickening and acting as an *in situ* forming drug delivery system. In this study, 2% mangostin was incorporated into poloxamer 407 and evaluated for antimicrobial activity against *Streptococcus mutans* KPSK₂ comparing to blank formulation, mangostin extract, 95% ethanol and 0.2% chlorhexidine.

After incubation, areas of inhibition zone were presented in all tested compounds except blank formulation. The diameters of inhibition zone are shown in Table 23. It was found that 0.2% chlorhexidine had the most inhibitory effect on *Streptococcus mutans* KPSK₂ and mangostin extract had a slightly higher effect than

the formulation. While 95% ethanol had a little effect on the antimicrobial activity which indicated that the inhibitory effect of mangostin came from itself. Blank formulation did not show zone of inhibition which meant there was no antimicrobial activity of poloxamer 407. These results indicated that mangostin incorporated into the formulation can diffuse into the medium at sufficient concentration for inhibition of the bacterial growth.

Table 23 Inhibition zone diameters of the test compounds on *Streptococcus mutans* KPSK₂

Test compounds	Inhibition zone diameter (mm)
Monoglyceride-based drug delivery system with mangostin	no
Monoglyceride-based drug delivery system without mangostin	no
Poloxamer 407 formulation with mangostin	13.33±0.29
Poloxamer 407 formulation without mangostin	no
Mangostin extract in 95% ethanol	15.33±0.29
0.2% chlorhexidine	24.00±0.00
95% ethanol	6.75±0.25

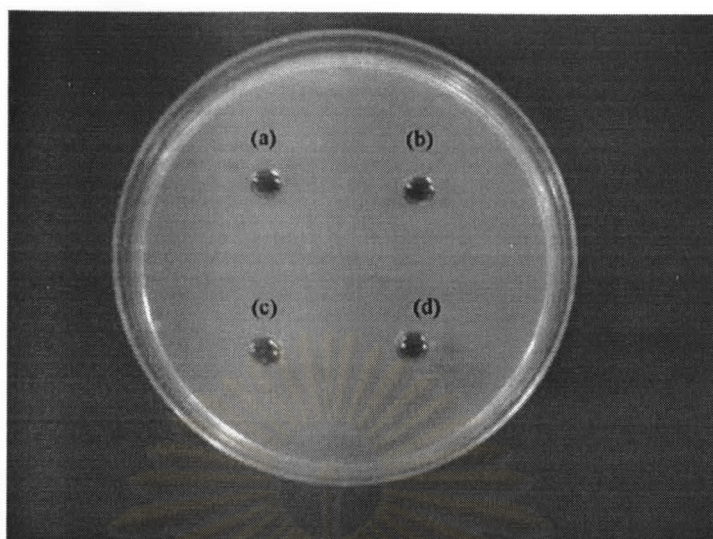


Figure 58 Agar diffusion test of monoglyceride-based drug delivery system; (a) and (b) monoglyceride-based drug delivery system with mangostin; (c) and (d) monoglyceride-based drug delivery system without mangostin

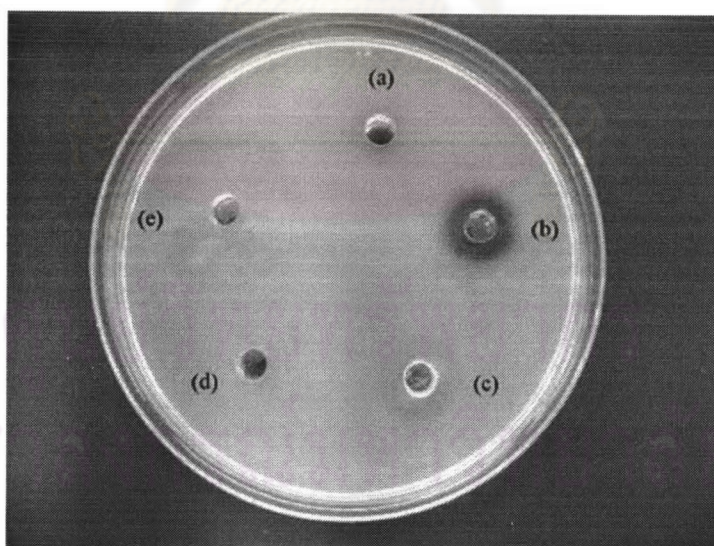


Figure 59 Agar diffusion test of various compounds; (a) poloxamer 407 formulation without mangostin; (b) poloxamer 407 formulation with mangostin; (c) mangostin extract; (d) 95% ethanol; and (e) 0.2% chlorhexidine

F. Determination of Partition Coefficient of *Garcinia mangostana* Extract

The lipophilicity of an organic compound is usually described in terms of a partition coefficient (P), which can be defined as the ratio of the equilibrium concentrations of a dissolved substance between organic and aqueous phases. There are many different techniques which can be used to solve this problem. The most common method is the shake flask method, the thorough mixing of the two phases followed by their separation in order to determine the equilibrium concentration for the substance being examined. The n-octanol-water system has been widely adopted as a model of the lipid phase. Lipophilic species dissolve in the aliphatic regions of the octanol, whilst hydrophilic species are drawn to the polar regions. The partition coefficient is usually given in a logarithmic scale, therefore, a $\log P = 0$ means that the compound is equally soluble in water and in the partitioning solvent. If the compound has a $\log P = 5$, then the compound is 100,000 times more soluble in the partitioning solvent. A $\log P = -2$ means that the compound is 100 times more soluble in water, i.e., it is quite hydrophilic.

In this study, the determination of partition coefficient was performed by the shake flask method. *Garcinia mangostana* extract was shaken between n-octanol and water layers, and then the adequate volume was withdrawn and analyzed by using UV spectrophotometry. As a result, the concentrations of mangostin in n-octanol and water phases were 4.7547 ± 0.3031 mg/ml and 0.0038 ± 0.0006 mg/ml, respectively. The partition coefficient is the quotient of two concentrations and is given in the form of its logarithm to base ten ($\log P$). Therefore, the partition coefficient and $\log P$ of mangostin were 1251.24 and 3.10, respectively. These data indicated that the compound was 1251.24 times more soluble in n-octanol than in water and it was quite lipophilic.

From the high partition coefficient of mangostin obtained from this study, it confirmed the result of the agar diffusion method (topic E6). Mangostin is highly lipophilic that the diffusion into the aqueous solid medium is negligible. Thus, the

antimicrobial activity of monoglyceride-based drug delivery system with mangostin could not be demonstrated.

G. Stability Study of *Garcinia mangostana* Extract Monoglyceride-Based Drug Delivery System

The stability study of *Garcinia mangostana* extract in monoglyceride-based drug delivery systems was performed by the stress condition using the heating-cooling cycle. The physicochemical properties and the amount of mangostin were determined at the initial time and after the stability study. The analytical method which employed in this investigation was the HPLC method as previously described.

As a result by visual inspection, the color change, phase separation and precipitation of all formulations were not observed after the heating-cooling cycle. The pH of formulations before and after the heating-cooling cycle were similar in the range of 5.64-5.85 and 5.70-5.83, respectively. The viscosity values of formulations were slightly decreased compared to those before the heat-cooling cycle. The polarizing microscopic images at the initial time and after the stability study were not different (Figures 60-61).

Table 24 pH and viscosity of formulation before and after stability study

Formulation	Before stability study		After stability study	
	pH	Viscosity (cps)	pH	Viscosity (cps)
1	5.78	5203.66	5.83	5055.42
2	5.79	5262.52	5.81	5007.46
3	5.64	5109.92	5.70	4944.24
4	5.85	4937.70	5.83	4796.00
5	5.81	4933.34	5.81	4743.68
6	5.64	4830.88	5.74	4691.36

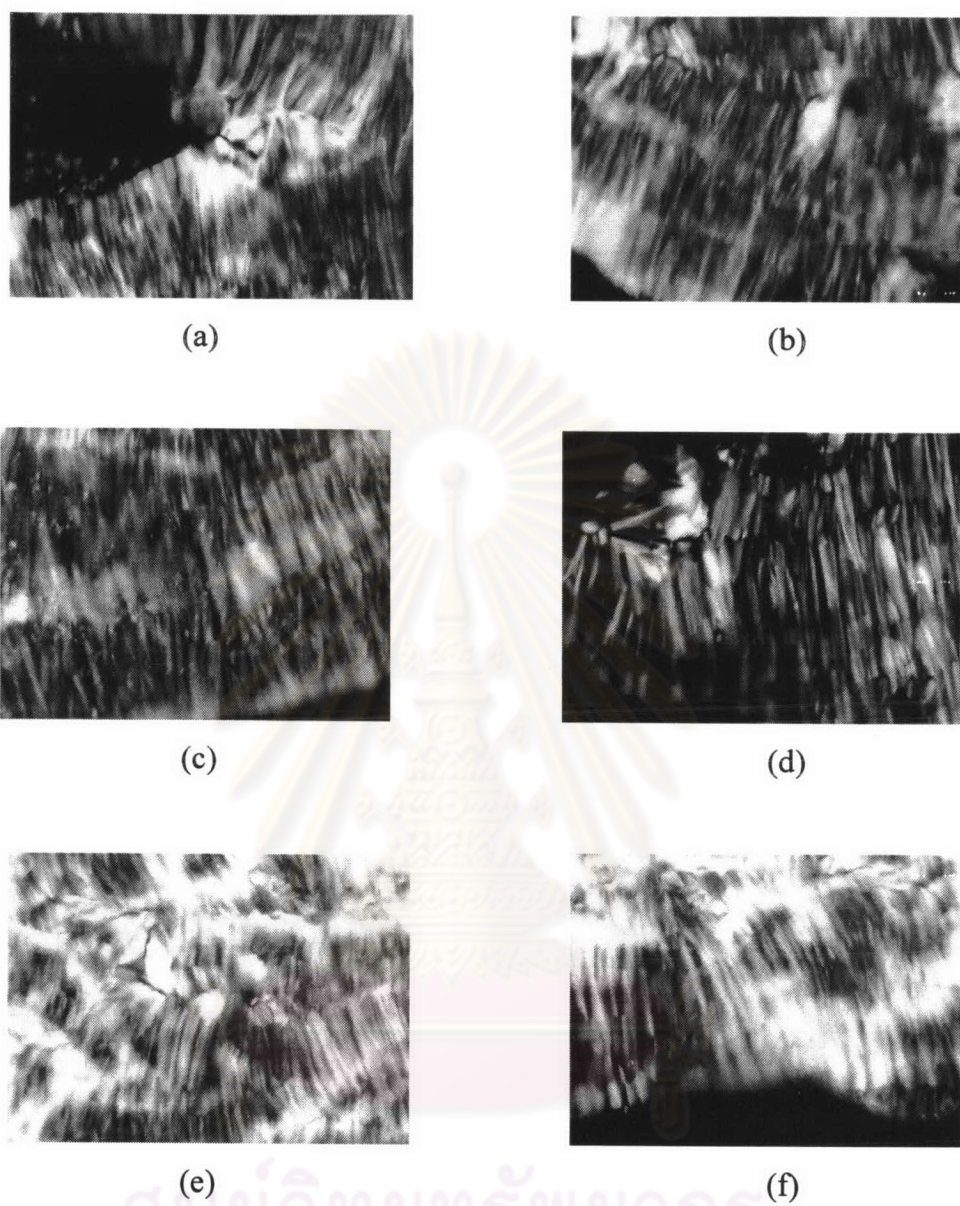


Figure 60 Polarizing microscopic images of formulation 1-3 before and after the stability study; (a) and (b) formulation 1; (c) and (d) formulation 2; and (e) and (f) formulation 3, as observed at $\times 100$ magnification

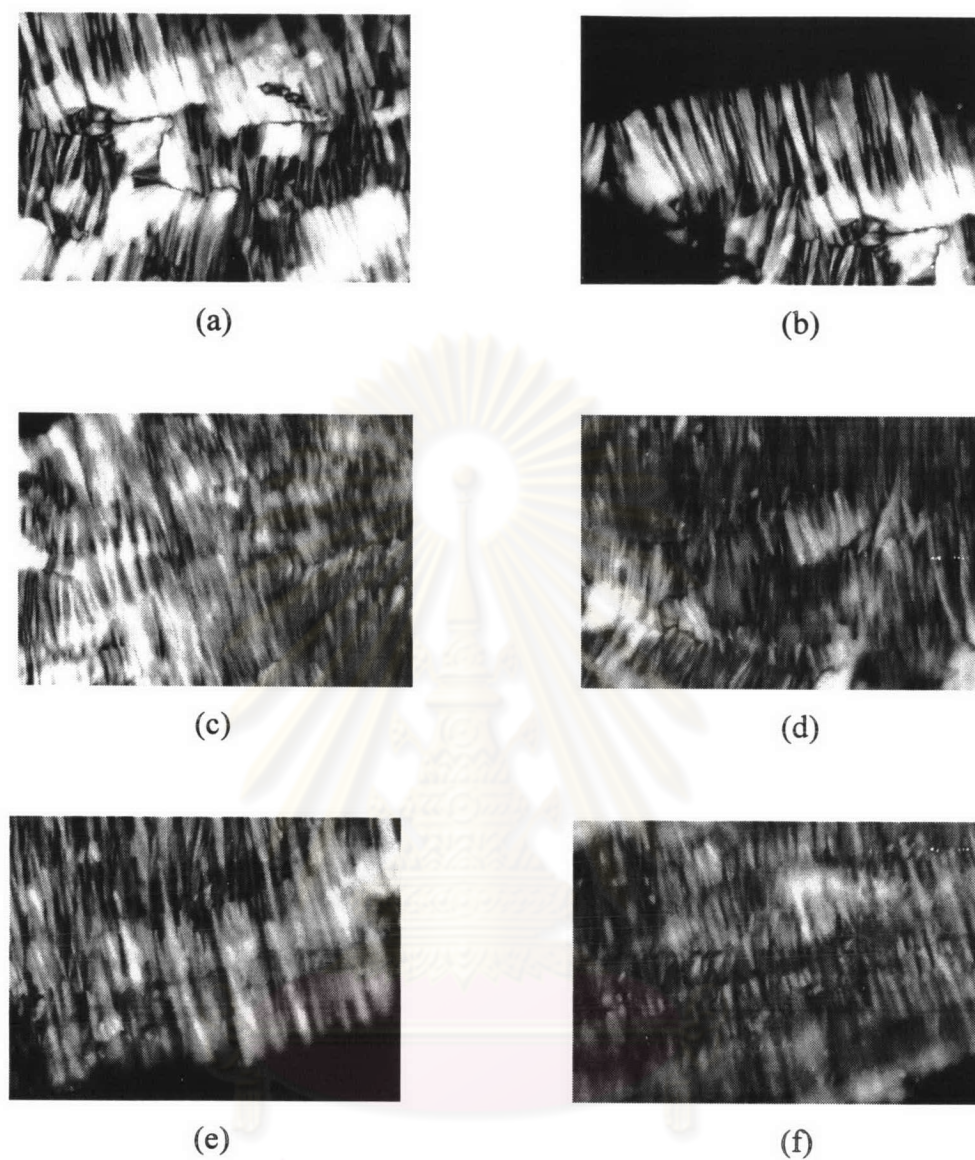


Figure 61 Polarizing microscopic images of formulation 4-6 before and after the stability study; (a) and (b) formulation 4; (c) and (d) formulation 5; and (e) and (f) formulation 6, as observed at $\times 100$ magnification

Since these formulations were expected to act as an *in situ* forming drug delivery system, therefore the low-viscous state formulations should be considered. In this study, the formulations both low-viscous state and high-viscous liquid crystalline phase were analyzed the amount of mangostin and calculated the percent remaining and percent loss of mangostin in monoglyceride-based drug delivery systems (Tables 25-26). Analysis of data indicated that the amount of mangostin in the formulations before and after the stability study were significantly different ($P < 0.05$) in both low-viscous state and high-viscous liquid crystalline phase, however all formulations appeared to be stable due to their percentage loss after storage was less than 10% of the initial value. In addition, there was no statistically significant difference ($P > 0.05$) in amount of mangostin remaining between six formulations both low-viscous state and high-viscous liquid crystalline phase.

Table 25 Amount of mangostin in low-viscous state formulation before and after stability study

Formulation	Amount of mangostin (mg)		Percent remaining of mangostin	Percent loss of mangostin
	Before	After		
1	19.92±0.24	19.68±0.28	98.80±1.39	1.20
2	19.93±0.19	19.66±0.15	98.65±0.73	1.35
3	20.02±0.26	19.78±0.16	98.81±0.82	1.19
4	19.85±0.29	19.65±0.21	99.00±1.07	1.00
5	20.01±0.20	19.71±0.18	98.48±0.92	1.52
6	19.95±0.25	19.78±0.23	99.18±1.15	0.82

Table 26 Amount of mangostin in high-viscous liquid crystalline phase formulation before and after stability study

Formulation	Amount of mangostin (mg)		Percent remaining of mangostin	Percent loss of mangostin
	Before	After		
1	20.01±0.17	19.73±0.19	98.59±0.95	1.41
2	19.93±0.24	19.68±0.35	98.73±1.76	1.27
3	19.98±0.20	19.67±0.50	98.45±2.48	1.55
4	19.97±0.30	19.67±0.47	98.54±2.33	1.46
5	19.90±0.35	19.73±0.55	99.12±2.77	0.88
6	20.03±0.42	19.60±0.47	97.81±2.33	2.19

ศูนย์วิจัยทรัพยากร
จุฬาลงกรณ์มหาวิทยาลัย